UNIVERSITY OF CALIFORNIA, SAN DIEGO

Processes Affecting the Spatial and Temporal Variability of Methane in a Temperate Dammed River System

A thesis submitted in partial satisfaction of the requirements for the degree Master of Science

in

Earth Sciences

by

Nicole A. Bilsley

Committee in charge:

Professor Miriam Kastner, Chair
Professor Neal Driscoll
Professor Jeffrey Gee

2012

The Thesis of Nicole A. Bilsley is approved, and it is acceptable in quality and form for publication on microfilm and electronically:

_____

_____

_____

Chair

University of California, San Diego

2012

DEDICATION

I would like to dedicate this thesis to my family, who has been an endless supply of support and encouragement throughout my life.

TABLE OF CONTENTS

LIST OF ABBREVIATIONS

ICOLD……International Commission on Large Dams

IPCC……...Intergovernmental Panel on Climate Change

BCRR……..Bernet Catch Regional Report

FID-GC……..Flame Ionization Detector Gas Chromatograph

mbsl……..meters below sea level

LIST OF FIGURES

LIST OF TABLES

ACKNOWLEDGEMENTS

I cannot express enough the appreciation I have for my advisor, Prof. Miriam Kastner. Over the last three years, she has gone above and beyond the role expected of an advisor. The experiences and opportunities she has provided me with, from attending conferences and meetings to participating on cruises and diving in Alvin, have truly shaped the time I have had at UCSD and have taught me lessons that will stay with me for the rest of my life.

My committee members, Prof. Neal Driscoll and Prof. Jeffrey Gee, have also played vital roles in my time at UCSD. They both taught classes that influenced my decision to switch to the Environmental Systems Earth Science track in Fall Quarter 2008. Thank you both for your enthusiasm, encouragement, and mentoring during classes, fieldtrips, cruises, and conferences over the last few years.

Special thanks go to Dr. Daniel McGinnis, who provided me with the opportunity of working on this project. Thank you for giving me a chance when I emailed you three years ago, without your trust and guidance I would never have had the incredible experience of working on this project and living in Germany.

I would like to express significant gratitude to Dr. Mark Schmidt, who has been my mentor on the Schwentine Project over the last year. Thank you for your patience with me when I knocked on your office door every day with questions, and your constant support and guidance.

I also thank the team at CONTROS SYSTEMS & SOLUTIONS. Not only did you teach me a large portion of the technical knowledge needed for this

project, but you also welcomed me into your community and made me feel at home. I look forward to future meetings and collaboration.

Huge thanks go to the laboratory at IFM-Geomar. The project could not have been completed without the technical expertise, guidance, and hard work of technicians and interns. I would like to sincerely thank Bettina Domeyer, Hans Cordt, Peggy Wefers, Stefanie Walther, and Abdurahman Aljuhany for their support.

Thank you to the Environmental Systems and Earth Science Departments, who have been a constant support system over the last seven years. Jane Teranes, Pam Buaas, Caren Duncanson, and Josh Reeves: you have been vital to my success and experience at UCSD and I cannot thank you enough.

Thank you to Andreas Maeck and Sabine Flury-McGinnis for their extensive support and participation in the August 2011 campaign sample collection and analysis, as well as with assisting with calculations.

Thank you to Lorenzo Rovelli for assistance with program and sensor training.

Thank you to Hans-Jürgen Weber of the Ministerium für Energiewende, Landwirtschaft, Umwelt und ländliche Räume for assistance with river flow data, and Frauke Nevoigt of IFM-Geomar for assistance with weather data.

Thank you to Schwentinetalfahrt, who provided continuous support throughout the extent of the project with canoe rentals, electricity supply, and logistics.

Funding for this work was provided by the German Research Foundation DFG Grant No. MC 214/1-1

This project was a large collaborative effort, and only a few of the team members are specifically listed here. I would like to extend extreme gratitude to everybody who provided physical and moral support to this project who is not mentioned. This project would not have been possible without you.

ABSTRACT OF THE THESIS

Processes Affecting the Spatial and Temporal Variability of Methane in a Temperate Dammed River System

by

Nicole April Bilsley

Master of Science in Earth Sciences

University of California, San Diego, 2012

Professor Miriam Kastner, Chair

Research on the role of rivers as a significant methane source to coastal waters and the atmosphere has previously focused on tropical regions. This study attempted to understand the spatial and temporal variability of methane within a dammed temperate river system in northern Germany, and the river's methane contribution to the atmosphere and coastal waters. Dissolved methane and dissolved oxygen were routinely sampled from the dam to 3.2km upstream.

The sediment pore water methane was measured, as well as the atmospheric methane flux from the river. A 22 hour study was performed to understand the diurnal variability of methane in the river. To determine the spatial variability of methane in the Brackish Discharge Zone, the water column and pore water were analyzed for methane concentration. Methane concentrations in the river were supersaturated with respect to the atmosphere, reaching concentrations between 311-2257 ± 51nM and saturation ratios (*R*) from 62-451. It appeared that methane concentrations increased downstream as a result of methane accumulating from runoff. Precipitation-induced runoff and dam opening were found to be the dominant factors affecting the overall river temporal methane variability. The dam outlet caused a significant degassing methane flux, from 5-25% of the methane concentration immediately before the dam. In coastal waters near the dam, the river was the dominant methane source, contributing 2.1–4.5kg CH_4/day. This study suggests temperate rivers, especially those which are dammed, may need to be considered when constraining coastal and atmospheric methane budgets.

CHAPTER 1: INTRODUCTION

Since global climate change has become a pressing international concern over the last few decades a significant effort has been made to understand the global budget of greenhouse gases, particularly the inputs and outputs of methane and carbon dioxide to and from the atmosphere. Studies have attempted to constrain the magnitude of the contribution of these gases from natural as well as anthropogenic sources (Khalil and Rasmussen, 1983). However, researchers have struggled to constrain the global methane contribution of freshwater bodies to the atmosphere (Bastviken et al. 2004, Bastviken et al. 2011) and coastal waters (Scranton and McShane, 1991, Bange et al. 1994). Freshwater studies are scarce, and the majority of those performed has been focused on tropical regions (Galy-Lacaux et al. 1999, Abril et al. 2005) due to the high productivity and size of rivers there. In addition, the effect of large dams on methane accumulation in the water column and flux to the atmosphere via ebullition, diffusion, and degassing at dam outlets is not thoroughly understood and has become a concern.

The International Commission on Large Dams (ICOLD, 2003) maintains a record of large dams greater than 15m high in size. Lima et al. 2008 estimated that these large dams may emit a total of 104 ± 7.2Tg CH_4/year to the atmosphere from turbines, spillways, and reservoir surfaces. This is considerable, as total methane emissions (natural and anthropogenic) to the atmosphere have been estimated to be between 485-550Tg CH_4/year (Lima et al. 2008). Emissions from rivers in temperate regions (between >54°–66°

latitude) have been estimated to account for only ~1% of these freshwater emissions (Bastviken et al. 2011). Emissions from temperate rivers and small dams have often been considered negligible, leading to a significant lack of knowledge of methane contribution from these regions. In addition, the methane concentration studies in temperate rivers that do exist have yielded highly variable results. This preliminary study attempted to build upon the limited existing research of temperate water systems by analyzing a small dammed freshwater river in Northern Germany.

CHAPTER 2: OBJECTIVE AND SUMMARY OF RESEARCH

The main goal of this study was to better understand the influence dams have on methane concentrations in freshwater river systems and the contribution of these systems to methane in coastal waters and the atmosphere. In addition, an attempt was made to understand the dominant factors affecting the spatial and temporal variability of methane in the Schwentine River. Three sections of the system were analyzed, including the river, the dam outlet, and the Brackish Discharge Zone where the river flows into the ocean. In the river, the summer spatial and temporal variability of methane concentration was determined. Methane concentration was correlated with weather factors, river flow rate, and dissolved oxygen to determine any potential relationship with the temporal variability of methane in the river. The influence of vigorous mixing within the dam outlet on the methane flux to the atmosphere and coastal outflow was determined. In the Brackish Discharge Zone, the goal was to understand the contribution of methane from the river discharge. This study contributes to the understanding of global methane budgets, and provides insight on the emissions from small dammed rivers in temperate regions.

CHAPTER 3: BACKGROUND

Methane is a potent greenhouse gas, contributing up to 15% of the current greenhouse effect (Houghton et al. 1990). It is roughly 24 times more effective in trapping heat in the atmosphere than CO_2, and is considered a significant player in climate change. The Intergovernmental Panel on Climate Change (IPCC) Assessment Synthesis Report released in 2007 reported that since pre-industrial times, the concentration of methane has increased in the atmosphere from 715ppb to 1,774ppb in 2005 (Pachauri and Reisinger, 2007). The IPCC Report in 2007 stated that this increase in methane concentration is likely to be the result of fossil fuel use and agriculture. Scientists have placed significant efforts in identifying and constraining the magnitude of methane sources to the atmosphere to understand the pre-industrial as well as the current methane budget. The IPCC Report 2007 summarized the magnitude of natural and anthropogenic sources and sinks of methane. Natural wetlands are considered to be the largest natural sources of methane to the atmosphere, with the southern and tropical regions accounting for 70% of these emissions (Pachauri and Reisinger, 2007). Many factors lead to high variability in methane concentrations and emissions in freshwater bodies; however the extent of their impact is weakly understood. Runoff has been shown to significantly affect methane concentrations in rivers. Agricultural runoff often contains methane from the waste of ruminants as well as may facilitate anaerobic decomposition due to high nutrient concentrations. In addition, recent research has shown that methane released from degassing at dams (Fearnside, 2002, 2004, 2005a, 2005b) creates

a significant methane flux to the atmosphere. The dominant factors affecting methane concentrations in freshwater bodies must be explored to better understand the impact these systems have on global methane budgets.

Data of surface water methane concentrations and atmospheric emissions have been relatively scant, highly variable, and understudied in many parts of the world. Swinnerton et al. 1969 was one of the first studies to measure methane concentrations in a river surface. They measured surface water concentration in the Potomac River, United States to be from 4 to 5 $x10^{-5}$ml/l CH_4, and attributed the variability in methane concentration to pollution discharge into the river. Wilkniss et al. 1978 measured methane concentrations at the Sepik River and nearby coast in Papua New Guinea. Concentrations measured at noon in the river ranged from 196-290ml/l CH_4, and represent concentrations in a river uninfluenced by anthropogenic activity.

Zimmerman 1977 was one of the first studies that calculated surface fresh water methane fluxes to the atmosphere. In the Florida canal and estuary, they estimated that canals and streams contribute an average of 140mg CH_4/m^2day, and that the estuary contributes an average flux of 10mg CH_4/m^2day.

De Angelis and Lilley 1987 added to the surface water methane data by studying various river and estuarine areas in Oregon over a four year period. They found that methane concentrations ranged from 4.8-1,730nM with saturation ratios (*R*) from 2-598. The origin of the methane was not clear in this study; however, the high concentrations in anthropogenically perturbed rivers were attributed to runoff from fertilized soils. Unperturbed rivers, on the other

hand, were able to reach high methane concentrations similar to polluted rivers. They suggest that most of the methane in unperturbed rivers originates from natural runoff from forest and agricultural soils as well as lateral diffusion from stream banks, although methane may also come from methanogenesis in the sediment.

The high methane concentrations measured in freshwater river systems have inspired research investigating the sources and sinks of methane to the water column and atmosphere. Bastviken et al. 2004 demonstrated that methane emissions from freshwater bodies to the atmosphere can be emitted via diffusion, ebullition, as well as plant-mediated transport. They compiled the total inland water methane emissions from lakes, reservoirs, and rivers, and published an emission estimate of 103Tg CH_4/year from these sources. They measured emissions from eleven North American and thirteen Swedish lakes. Compounding this data with data from forty nine additional lakes, they estimated that lakes globally contribute 8–48Tg CH_4/yr, or 6–16% of total natural methane emissions. They assumed when calculating the percent contribution of methane from lakes that the average and maximum of total natural methane emissions was 145 and 304Tg CH_4/year, respectively (Wuebbles and Hayhoe, 2002). This large range of lake emissions supports the need to study methane dynamics in more freshwater bodies. In addition, this high flux shows the potential for freshwater bodies to be a significant contributor of methane to the atmosphere.

Further research has been done in an effort to quantify how much methane actually reaches the atmosphere by ebullition. McGinnis et al. 2006

modeled the diffusion of methane across the bubble-water interface in marine environments. These models were further modified by Del Sontro et al. 2010 for the freshwater environment at Lake Wohlen, a 90 year old hydropower reservoir in Switzerland. They found approximately 70% of the methane in a pure methane model bubble would reach the surface and be emitted to the atmosphere. The remaining 30% would dissolve into the water column as the bubble ascended. These results were generated by capturing bubbles in gas traps placed at water depths between 2-16.5m. Oxidation experiments suggested that no significant oxidation occurred in the water column. Through the use of these bubble traps suspended in the water column, air collection chambers at the water surface, water sampling in the water column and pore water, and bubble modeling they constrained the sources and sinks of methane into the reservoir. They concluded that the methane emissions from temperate water bodies should be considered in greenhouse gas budgets.

Understanding the sources of methane to coastal waters is important in terms of hydrocarbon exploration along the coast, as well as for fluxes of methane to the atmosphere from the ocean. Scranton and McShane, 1991 showed that freshwater river discharge into the North Sea may be a significant source of methane to coastal waters. In the open North Sea, methane concentrations were close to or at equilibrium with the atmosphere. However, at the river discharge zones, the water reached up to 120 times saturation with respect to the atmosphere (Scranton and McShane, 1991). They concluded that rivers globally contribute less than 0.2% of the global emissions to the

atmosphere. However, rivers are a significant source of methane to coastal waters. Scranton and McShane, 1991 noted that the one of the largest uncertainties in their data was the lack of knowledge of methane distribution in the river and coastal waters. This thesis attempted to broaden the understanding of the spatial variability of methane in a river and the coastal waters at the river's mouth.

Coastal marine methane fluxes to the atmosphere have become a more prominent concern as the sources and sinks of methane are being constrained. The ocean only accounts for ~2% of natural and anthropogenic sources of methane to the atmosphere combined (Cicerone and Oremland, 1988). Bange et al. 1994 found that in the Baltic and North seas, the shelf region and estuaries contribute approximately 75% of these global oceanic emissions. Since the shelf and estuaries appear to be the dominant source of oceanic emissions, it is important to understand how much of this methane is coming from freshwater river sources. This thesis attempted to quantify the amount of methane contribution from a river to the coastal waters.

When these freshwater systems are dammed, methane fluxes from the water to the atmosphere may be enhanced by the aeration at the dam outlet. These aeration systems within the dam are typically put in place to reduce the oxygen consumed during methane oxidation in the discharge waters. Although the extent to which degassing of methane occurs depends on water turbulence, several studies have generated estimates by processing samples for methane concentration analysis before and after a dam outlet. A study by Galy-Lacaux et

al. 1997 determined that approximately 80% of the methane in the water is degassed at an aerating weir at Petit Saut, French Guiana. Galy-Lacaux et al. 1999 claim that ebullition and diffusion from the river also play an important role in methane emissions during the first three years after impoundment of the river, however the dominant methane emission process to the atmosphere is from degassing at the dam outlet and from a change in river flow and morphology downstream of the dam. Abril et al. 2005 found that approximately 60% of the total methane flux of the river system comes from degassing at the dam. Although these estimates are highly variable as a result of solubility conditions, the degree of turbulence, and the stream morphology, it is important to understand the range at which aeration at a dam can influence methane flux from the water to the atmosphere.

This study in the Schwentine River furthers understanding of the driving factors influencing the spatial and temporal variability of methane in a temperate freshwater river system. The effect of the dam and outlet on surface water methane concentration, atmospheric methane flux, and discharge into the fjord was explored. In addition, this study attempted to better understand the sources of methane to the Schwentine and the estimated methane contribution of this river to the coastal waters in the Baltic Sea.

CHAPTER 4: STUDY AREA

The Schwentine is a 70km long freshwater river of the Schlei/Trave river basin in Northern Germany (Figure 1). Its source is in Bungsberg, and it passes through 22 lakes before emptying in the Kiel Fjord, Baltic Sea. The lakes have been classified by the Bernet Catch Regional Report (Bernet Catch Regional Report, 2006) as consisting of calcium rich waters, large and small river basin sizes, and stratified and non-stratified lakes. The Schwentine river basin is characterized by agricultural as well as residential land. The river is also home to a boating company which ferries visitors up and down the most downstream 6 kilometers of the Schwentine multiple times per day. The Schwentine is fed by numerous small drainage channels in the river's 726km² sub-basin, contributing runoff water to the river (Bernet Catch Regional Report, 2006). The river basin size is 457km^2, and collects runoff from the surrounding land at rates of 4.38m^3/s or 9.58l/(skm^2) (Bernet Catch Regional Report, 2006). The BCRR classified the Schwentine as a combination of Type 16, 17, and 19 streams, defined as "gravel streams", "gravel rivers," and "partly-mineralic streams" (Bernet Catch Regional Report, 2006). Gravel streams and rivers have a gravel dominated bottom substrate. Partly-mineralic streams typically have an organic material dominated bottom and consist of both still and flowing segments (Brunke, 2004). Just before the river termination, a dam regulates the flow out to the coastal waters in the Kiel Fjord. This dam slows the velocity of the river downstream, and causes vigorous mixing of the river water at the outlet. The equilibrium solubility

concentration of methane in the river is approximately 5nM CH_4 (Duan and Mao, 2006). The equilibrium solubility concentration of methane in the Brackish Discharge Zone is approximately 4nM (Duan and Mao, 2006).

CHAPTER 5: SAMPLING STRATEGY

To capture the spatial and temporal variability of methane, sample sites were placed approximately 250-300m apart starting from the dam and continuing upstream (Figure 2). To determine the effect that mixing at the dam outlet has on methane concentration, one site (called 'Back Restaurant') was included after the dam at the entrance to the Brackish Discharge Zone. In 2010, nine sample sites in the river were distributed over 2480m upstream from the dam. The distance of each sample site from the dam is recorded in Table 1. Samples for methane and dissolved oxygen were taken weekly between July 21-September 14, 2010 (excluding three weeks in August), and two times a week between June 30-August 5, 2011. In 2011, the previous year's sites were re-occupied, as well as an additional sample site 3200m upstream from the dam (called 'Birdhouse Clearing', see Figure 2) and a sample site in a drainage channel outflow 3100m upstream from the dam (called 'Drainage Channel', see Figure 2). Samples for dissolved phosphorous were also taken on July 26, July 28, and August 2, 2011 to contrast nutrient concentrations in the river water with the concentrations in the drainage channel.

In addition to measurements in the river water, cores were taken for pore water analysis in 2010 and 2011. A core was taken 15m upstream from Bridge 1 (see Figure 2) on September 17, 2010 to determine the contribution of methane from the sediment. Cores were also taken in the river on August 18 and 19, 2011 at 2km and 1km (aerial distance) from Ladder 2 (see Figure 2), and approximately 100m from Ladder 2 in the small forebay area before the dam.

The river cores taken in 2011 are not reported here and will be included in a future study.

To understand the diurnal variability of methane concentration, samples were collected every 2-3 hours over a 22 hour period from August 17-18, 2011. Methane and dissolved oxygen samples in the water column were duplicated to calculate the analytical error.

A sampling survey was conducted on July 15, 2011 in the Brackish Discharge Zone of the Schwentine into the Kiel Fjord (Baltic Sea) to understand the distribution and dominant sources of methane in the coastal waters. Five locations were visited (see Figure 2). Water samples were taken 1m below the surface and 1.5m above the sediment-water interface. The water depth of each sample site is shown in Figure 3. Water temperature and salinity (via conductivity meter) were recorded, and water samples were taken for dissolved methane and dissolved oxygen analysis. Sediment push cores were taken at Sites 1, 2, and 4 shown in Figure 2.

CHAPTER 6: METHODOLOGY

The following Methodology sub-chapters are divided into sampling performed in the river and Brackish Discharge Zone. Sample site 'Back Restaurant' was sampled using the same methods as the river samples, despite that it was downstream of the dam. Methods for achieving flow rate data, weather records, and errors follow.

6.1: Sampling in River

6.1.1 Dissolved Methane in Water Column

Water samples collected for methane concentration analysis were analyzed using gas chromatography. During the river transects and a 22 hour survey, samples were taken 10cm below the water surface using 20ml glass vials. The filled vials were sealed with a rubber stopper and crimped with an aluminum cap. While the water was being collected, the vial faced upstream to allow the river water to completely flush through the vial and remove any potential contaminants acquired during vial transport. It was confirmed that the sample vials were bubble free to prevent equilibration with unwanted headspace. Within 1-3 hours after sampling, a 5ml N_2 headspace was added to the vials to create a headspace of known concentration. Nitrogen was used because it is not detected in a Finnigan TraceGC Ultra Flame Ionization Detector Gas Chromatograph (FID-GC). The gas syringe was flushed twice with the nitrogen gas before adding the headspace to prevent contamination. As the headspace was added, the displaced 5ml of water exited the vial through an open syringe.

To prevent headspace from escaping, the gas syringe was inserted to middle of the vial neck, and the open syringe was inserted to the vial bottom before the headspace was added to the vial. The samples were shaken and allowed to equilibrate upside down before further analysis. A FID-GC was used to measure methane concentration in the headspace. The FID-GC was calibrated daily using standards of 10ppm, 100ppm, and 1000ppm. A 100µl injection of each sample headspace was injected into the FID-GC to measure the methane concentration. In between samples the gas syringe was flushed four times with nitrogen gas to prevent contamination. Laboratory/sample temperature and air pressure were recorded for appropriate calculation of the concentration of CH_4 in the sample water. The water concentration corresponding to the concentration measured in the headspace was calculated using the Wiesenburg and Guinasso (1979) equation. Two different FID-GC's were used, one in 2010 and one in 2011. A comparison was done between the FID-GC's in 2010. The FID-GC used in the 2011 analysis generated results on average 115nM higher than the FID-GC used in 2010 (standard deviation of 36nM). The reason for this discrepancy is not known. The maximum error for the gas standards used to calibrate the FID-GC was 2.1ppm in 2011. The gas standard error in 2010 was not recorded, so the error for the 2011 gases was used in the error calculations.

6.1.2: Dissolved Oxygen in Water Column

In 2010, dissolved oxygen measurements were taken each sampling day at upstream and downstream locations ('River Center' or 'Flatdock', and 'Ladder

2' respectively.) The 2010 samples were taken 10 cm below the water surface, and tested immediately using an AquaMerck field titration kit. In 2011, dissolved oxygen measurements were taken at every sample site during river transects to determine if spatial variability exists. A different procedure was followed to measure dissolved oxygen concentration in 2011. Samples were collected with Winkler bottles of known volume at 10cm below the water surface. Bottles were faced upstream during sample collection to flush. 0.5ml of alkaline iodide and 0.5ml of manganese-II chloride were added to the sample to fix the oxygen. Vials were closed with a glass stopper and checked to make sure they were bubble free. Samples were shaken and sampled either immediately after collection or the following day in the laboratory. If samples were titrated the following day, they were stored under refrigeration to prevent microbial growth. 20ml of the sample solution was removed from each Winkler bottle to allow room for titration. 1ml of H_2SO_4 (9M) was added to the sample to dissolve the Mn-hydroxides. The sample was mixed using a magnetic stirrer to fully dissolve the complex. The solution was titrated with sodium thiosulfate (0.01M) until a light yellow color was achieved. 1ml of zinc iodide indicator was added to the sample before the solution was titrated to a clear, colorless liquid. The oxygen concentration was calculating using the following (IFM-Geomar Geobiochemical Analysis Online Resource):

Equation (1)

$$O_2\ [cm^3/l] = (0.5 * a * f * 0.112 * 10^3) / (b - 1)$$

a = comsumption of thiosulphate solution (cm^3)
b = volume of the sample bottle (cm^3)
f = *f*-factor of the thiosulfate solution

The *f*-factor was calculated through the calibration of the sodium thiosulfate solution prior to sample titration. $1cm^3$ H_2SO_4 (9M), $0.5cm^3$ alkaline iodide, and $0.5cm^3$ of Mn_2Cl were separately added to $50cm^3$ of Milli-Q water, and mixed. $10cm^3$ of iodate-standard was added. The solution was titrated with the 0.01M sodium thiosulfate solution until a light yellow color was achieved. $1cm^3$ zinc iodide solution was added, and the titration was continued until a clear colorless liquid was achieved. The *f*-factor was calculated using the following equation (IFM-Geomar Geobiochemical Analysis Online Resource)

Equation (2)

$$f = 10 / v$$

f = *f*-factor
v = consumption of sodium thiosulfate solution (in cm^3)

6.1.3: Dissolved Methane in Sediment Pore Water

1 push core was taken 15m upstream from the 'Bridge 1' sample site (Figure 2) on September 17, 2010. The core was in less than a meter water depth, and was 25cm long. Samples were taken for pore water methane analysis and porosity determination. The core liners were pre-drilled with 1cm holes at 1cm intervals. Sediment samples for methane analysis were taken with 3ml

open ended syringes pushed through these holes. These samples were placed in 20ml glass vials prefilled with 4ml NaOH solution, and closed with a rubber stopper and crimped aluminum cap. The methane in the headspace was measured using the process described above in the methane analysis procedure. It was assumed that all the methane in the pore water was released to the headspace as a result of the low solubility of methane in NaOH. The existing atmospheric methane concentration in the headspace was considered negligible. This core was taken to get a rough understanding of methane concentration in the pore water. No error analysis was performed.

Sediment samples for porosity determination were also taken with the 3mL open ended syringes and placed in pre-weighed jars. These samples were weighed, freeze dried, and weighed again to calculate the difference between the wet and dry weight. The volume of the pore water was calculated assuming 1g H_2O is equivalent to 1ml H_2O. The volume of pore water was used in the pore water methane concentration calculations. Data from the 2011 cores is excluded from this thesis but will be included in a future publication. The porosity calculation follows:

Equation (3)

$$PW = WS - DS$$

PW = mass of pore water (g)
WS = mass of wet sediment (g)
DS = mass of dry sediment (g)
1g H_2O ~ 1ml H_20
Volume of pore water (ml) ~ mass of pore water (g)

6.1.4: Dissolved Phosphate in Water Column

Dissolved phosphate was measured during three sampling days in 2011: July 26 and 28, August 2. Samples were filtered upon collection. The laboratory analysis followed the procedure described in the IFM-Geomar Geobiochemical Analysis Online Resource. Standards of 0, 0.536, 1.315, 2.63, 3.945, 5.26, and 10.52µM were used. 2ml of each standard or sample was added to their own respective vials. 3ml of pure water was added to make a 5mL solution with the sample. 0.1ml of ascorbic acid was added, followed by 0.1ml of heptamolybdate reagent. The vials were capped and shaken, and allowed to stand for 10 minutes. The absorbance was then measured in a photometer at 880nm to determine the concentration of phosphate in the samples. The standard error of this method is 0.02µM.

6.1.5: Diurnal Methane Study

A 22 hour survey, from August 17-18, 2011, was conducted to better understand the diurnal variability of methane. Two samples were taken in 20ml glass vials capped with a rubber stopper and crimped aluminum cap every two hours during the day and every 3 hours during the night at ‘Ladder 2’. A 5ml nitrogen headspace was added, the samples were allowed to equilibrate, and 100µl of the headspace was processed in the FID-GC. The methane analysis procedure previously described was followed.

6.1.6: Methane Flux from River to Atmosphere

In order to estimate how much methane is being released by diffusion and/or ebullition to the atmosphere, plastic gas collection boxes were deployed in August 2011 (Figure 4). Plastic collection boxes were modeled after those used by Bastviken et al. 2004. Equipment construction and sampling was performed by Andreas Maeck. Each unit consisted of two plastic boxes (open on bottom) connected to a metal frame (Figure 5). Each box had a 2mm polytetrafluoroethylene outlet tube with two three-way syringes. The units were placed upside down in the water at a level stable enough to ensure the unit would not be overturned by waves. The syringe was closed at the end of the polytetrafluorethylene tube to isolate the gas in the box from the atmosphere. The volume of air in the box was measured using a ruler. Unit locations were at 50m (Site A), 70m (Site B), and 100m (Site C) from the dam (Figure 4). The Site A collection boxes were deployed from 10:06 to 12:18, and 12:29 to 14:58 on August 18, Site B collection boxes from 18:10 to 19:57 on August 17, and Site C collection boxes from 16:55 to 19:51 on August 17, and 12:09 to 14:56 on August 18.

Air samples were extracted from the box immediately after deployment to measure the baseline atmospheric concentration and every 30-60 minutes after over a 2-3 hour period. Air samples were stored in 20ml vials filled with saturated NaCl solution. Prior to sampling, these vials were completely filled with saturated NaCl solution and capped with a rubber stopper and crimped aluminum cap. Air samples were taken from the box's outlet tube via a syringe. The air sample was injected into the NaCl solution filled vial, with an escape needle for the displaced

solution. The methane in the headspace of each vial was measured with a FID-GC. It was assumed that no methane dissolved into the NaCl solution, and that the concentration in the vial headspace was the same concentration as in the collection box.

6.2: Sampling in Brackish Discharge Zone

6.2.1: Dissolved Methane, Dissolved Oxygen, Temperature, and Salinity in Water Column

On July 15, 2011 five sample sites were visited in the Brackish Discharge Zone after the dam (Figure 2). Water samples were taken with a 5l niskin bottle at 1m below the surface, and 1.5m above the sediment water interface. With each niskin recovery, water temperature and salinity were recorded, and water samples were taken for dissolved methane and dissolved oxygen analysis. Water temperature was recorded using a hand-held probe. Salinity was measured using a conductivity meter. Dissolved oxygen samples were collected in glass Winkler bottles, and processed in the laboratory three days after sampling using the sodium thiosulfate titration method described above. For methane analysis, 20ml glass vials were filled without bubbles, capped with a rubber stopper, crimped with an aluminum cap, and stored upside down under refrigeration. Three days later, a 5ml nitrogen headspace was added and the solution was shaken to equilibrate. 100µl of the headspace was analyzed for methane in a FID-GC.

6.2.2: Dissolved Methane in Sediment Pore Water

The three push cores measuring 16cm, 44cm, and 40cm respectively, were retrieved in the Brackish Discharge Zone (Figure 2). The core liner was deployed using a winch and gravity weights. Once on board, the core was slowly pushed out the top of the vertically held liner using a wooden plunger. Cores were sampled in approximately 5cm intervals in Core 1 (Site 1), and 10cm intervals in Core 2 (Site 2) and Core 3 (Site 4). Samples were taken to determine porosity and methane concentration in the pore water.

Porosity samples were taken by placing approximately 6-10g of sediment from a defined interval in the core into a jar of known weight. The samples were then weighed in the laboratory, frozen, freeze dried, and weighed again to find the water weight in the sample and porosity of the sediment. The volume of the pore water in the sediment samples were calculated using the previously discussed equation (3).

Samples for pore water methane analysis were collected using a 3ml open ended syringe. 3ml of sediment was placed into a 20ml glass vial prefilled with a 5ml NaCl saturated solution, capped with a rubber stopper and crimped shut with an aluminum cap. NaCl saturated solution was added to move the methane from the pore water into the headspace. The samples were stored for 3 days under refrigeration, equilibrated to room temperature, and shaken before sampling. The atmospheric methane was assumed negligible, and all of the methane in the pore water was assumed to have moved to the headspace. The volume of the pore water was measured using equation (3). The headspace

volume was determined by subtracting the volume of the wet vial contents from the total 20ml vial volume. The volume of the contents was found by assuming 1g of the contents was equivalent to 1ml. The calculation follows:

Equation (4)

$$V_{headspace} = V_{vial} - V_{sediment + pore\ water + NaCl\ solution}$$

$V_{headspace}$ = Volume of headspace
V_{vial} = Volume of vial (20ml)
$V_{sediment + pore\ water + HCl\ solution}$ = Volume of sediment, pore water, and NaCl solution

The concentration of dissolved methane in the pore water was determined using a FID-GC.

Samples for ion chromatography were also taken in the cores by use of rhizons (Seeberg-Elverfeldt et al. 2005). The rhizons were inserted into the sediment to retrieve pore water. The pore water was tested for sulfate and chloride ion concentration. These values will be reported and explored further in a future publication. The chloride ion concentration was used to calculate salinity using the following (IFM-Geomar Geobiochemical Analysis Online Resource):

Equation (5)

$$S = (Cl^- \text{ g/kg}) * 1.81537$$

S = Salinity (PSU)

6.3: Flow and Weather Records

River flow rate and weather data are available for comparison. Daily average river flow rates were taken at Oppendorf (near the 'Bridge 2' sample site shown in Figure 2) by the Schleswig-Holstein Agency for Coastal Defense. Our research group also measured flow closer to the dam, at the 'Last Bridge' sample site (Figure 2), by taking the cross sectional area across the river, and measuring the river velocity using the following methods. The cross sectional area was measured using an extendable meter stick. The velocity was found by recording the time it took oranges to move down the river. Each orange's velocity was measured over a 29.5m distance. Oranges were chosen because they float just below the water surface, minimizing the effect of wind drag. A total of six oranges were used for this study. The velocity of three oranges were averaged and used to calculate the river flow. The three remaining orange velocities were discarded as a result of path disturbance from a duck, a boat, and vegetation.

Weather data were provided by the IFM-Geomar weather records and the Deutscher Wetterdienst. Data for the wind direction at 40.5m, wind speed at 36m, and incoming short wave solar irradiance at 35m were retrieved from the IFM-Geomar weather records. The daily average precipitation was retrieved from the Deutscher Wetterdienst. The wind speed, solar irradiance, and precipitation values were recorded every 8 minutes. Wind speed was averaged from midnight to noon on each sample day. The water temperature used was the average of 6-10 measurements taken during the sampling period each sample day. The total

daily precipitation was recorded. The shortwave solar irradiance was recorded at noon on each sample day.

6.4: Calculating Errors

For the methane samples taken in the river in 2011, the analytical error was calculated by averaging the two samples (one duplicate) taken at each site, and taking the largest absolute difference between the average and one of the samples of the pair. The ranges of error for all the duplicate sample sets were averaged to achieve an overall analytical error of 16nM. The standard error was converted from the standard gas error of 2.1ppm, to 31nM, using the average temperature and salinity of the samples of 25℃ and 0PSU, respectively, as well as the sample and headspace volume of 15ml and 5ml, respectively.

The analytical error for the river methane samples in 2010 was performed in the same way, yielding an error of 20nM. However, the standard error of the gases was not recorded. Therefore, the standard error of 31nM from 2011 is used.

The error for the dissolved oxygen samples in 2010 and 2011 was calculated using the same method as the methane errors, averaging the range of error between percent saturation values of duplicate samples. The analytical error was 1% saturation in 2010, and 2% saturation in 2011. In 2010, samples taken on September 3, 7 (excluding ‘Flatdock’ measurement), and 14 were included in the error calculation, because they were the only dissolved oxygen samples taken that year with duplicates.

CHAPTER 7: RESULTS

7.1: Spatial Variability of Methane in River

Methane concentrations in the river water significantly increased downstream toward the dam in the 2010 and 2011 data sets, as shown in Figures 6 and 7, respectively. Concentrations in the river overall varied from 311–2257 ± 51nM CH_4 in 2010 and 386–1518 ± 47nM CH_4 in 2011. The saturation ratios varied from 62 to 451. The equilibrium solubility of the river water was assumed to be approximately 5nM CH_4 (Duan and Mao, 2006).

The concentration increase between sample sites increased downstream for every meter the river travels as shown in Figure 8 for 2011. There was a drop in the concentration added to the river water per meter the river traveled immediately before the dam. This may have been due to an increase in flow as the water exited through the dam, but it is not certain.

7.2: Temporal Variability of Methane in River

During the 22 hour survey, methane showed significant diurnal variability in concentration (Figure 9). It should be noted that the samples taken at 23:30 and 2:30 may have a larger margin of error, as there were small bubbles in the sample bottles. Unfortunately, the magnitude of error is unknown since the duplicate samples had bubbles as well. This may have caused the water to equilibrate with the bubble headspace, giving a lower methane concentration than the initial concentration in the water. This is because the water was likely supersaturated with respect to the atmosphere, and would have diffused to the

headspace bubble present in the vial. A peak in methane concentration in the diurnal cycle was seen at 15:20 and 23:30. A trough was seen at 20:15 and 5:30. The peak at 23:30 is not an artifact resulting from the bubbles in the sample vials because the peak was also seen in sensor data that will be published in a future study. However, the two samples taken before the nighttime peak had low concentrations that corresponding with an increase in flow rate. The overall peak in the daytime and trough in the nighttime follows closely after the daytime peak and nighttime trough in air temperature as well as solar irradiance (Figure 10).

There was strong temporal variability during the sampling season in the methane concentration of the river in 2011. The concentrations at each sample site in the river appeared to shift to higher or lower concentrations uniformly depending on the sample day (Figure 11). This suggests there was a dominant factor affecting the overall methane concentration in the stream relatively uniformly. These dominant factors were runoff into the river as well as the opening of the dam previously discussed. These factors will be further addressed later.

7.3: Correlating Weather Factors with Average Methane Concentration in River

The average methane concentration in the river for each sample day was correlated with various weather factors to determine if weather drove the uniform shift, seen in Figure 11, in methane concentration at all sites in the river from sample day to sample day. The weather factors included average wind speed,

water temperature, and precipitation. A strong correlation was seen in 2010 of methane concentration with water temperature (Figure 12). However, this correlation was not seen in 2011 (Figure 12). No correlation was seen with wind speed (Figure 13). A positive correlation of methane with precipitation was seen, having an r^2=0.68 (Figure 14). When flow rate was plotted with the temporal variability of methane over the sampling season previously shown in Figure 11, the flow data appeared to peak and trough with the overall methane concentration of the river (Figure 15). When the daily average river concentration was plotted with the river flow rate and precipitation, it was seen that large precipitation events preceded the peak in flow rate which coincided with the peak in methane concentration in the river (Figure 16).

7.4: Dissolved Oxygen in River

Dissolved oxygen varied between 83-121 ± 1% saturation in 2010, and 69-104 ± 2% saturation in 2011. There appeared to be a weak inverse correlation between methane and dissolved oxygen in 2010, however not in 2011 (Figure 17). In 2011, there does not appear to be any consistent spatial trend of dissolved oxygen downstream (Figure 18). Too few sample sites were used in 2010 to determine any spatial variability in dissolved oxygen. There is consistent temporal variability between sampling days in 2010 (Figure 19) and 2011 (Figure 20). The dissolved oxygen concentrations at the sample sites appear to vary consistently relative to each other from sample day to sample day, similar to the methane concentration (Figure 11). The water occasionally became

supersaturated with oxygen, likely because of aeration by turbulence or increased photosynthesis.

7.5: Dissolved Phosphate in River

Dissolved phosphate was measured over three sample days in 2011 to better understand the nutrient load in the stream and input from agricultural runoff. Within the river, phosphate concentrations ranged from 1.693-2.325 ± 0.02µM. Phosphate concentrations do not vary significantly downstream (Figure 21).

7.6: Drainage Outlet Chemistry

On July 28, August 2, and August 5, 2011, the outflow in a drainage channel (site 'Drainage Channel' shown on Figure 2) was sampled for methane. The drainage water there exited out of a pipe, and was likely the runoff from the agricultural land surrounding the river. The methane concentrations were very high on each sample day, at 1.4, 5.1, and 19.1 ± 0.3 µM, respectively. Dissolved oxygen and dissolved phosphorous were also measured on July 28 and August 2. The dissolved oxygen was low, at 77 ± 0.42% and 83 ± 0.23% saturation, in comparison to the rest of the river. The dissolved phosphorous was very high compared to the rest of the river, ranging between 8.1 and 8.4 ± 0.02 µM. The drainage water was 4.4℃ colder than the next upstream sample site 'Birdhouse Clearing' on July 28 and August 2, 2011, and 2℃ colder on August 5, 2011. The channel water was not well mixed with the river water, as seen by the large

difference in temperature, phosphorous, oxygen, and methane between the two waters, and the relatively stagnant appearance.

7.7: Contribution of Methane to River from Sediment Pore Water

The one core taken in the river in 2010 reached a maximum methane concentration of 941µM. No duplicate sample was taken at the same depth and the standard error was not recorded, so the error could not be calculated. The concentration profile down core can be seen in Figure 22 (assistance with calculations courtesy of Dr. Sabine Flury-McGinnis). This core was difficult to acquire due to the gravelly sediment, and should only be considered as a rough approximation to how much methane is present in the river sediment. Three additional cores were taken in the river to determine if the production of methane in the sediment changed downstream. This data will not be discussed here and will be presented in a future publication. A flux to the water column estimate was not calculated at this time due to limited data.

7.8: Methane Contribution of River to Atmosphere before Dam

Flux from the river to the atmosphere via ebullition and/or diffusion was calculated by the increase in concentration in the gas collection boxes. At Site A (Figure 4), the flux ranged from 0.29-55.1mg CH_4/m^2day. At Site B, the flux ranged from 0.65–3.98mg CH_4/m^2day. At Site C, the flux ranged from 0.45-59.34mg CH_4/m^2day. The average and range of these fluxes is displayed in Figure 23. The standard deviation is reported in Table 13. The flux

measurements were calculated (with assistance from Andreas Maeck) using the following equations:

Equation (6)

$$F_{\text{river to atm ppm/min}} = ([CH_4]_x - [CH_4]_y) / (x - y)$$

$F_{\text{river to atm ppm/min}}$ = Flux of methane from river to atmosphere (ppm/min)
$[CH_4]_x$ = Methane concentration at time x in box (ppm)
$[CH_4]_y$ = Methane concentration at time y in box (ppm)
x – y = difference between time x and time y (min)

Equation (7)

$$F_{\text{river to atm mol/min}} = (F_{\text{river to atm ppm/min}}) * 10^{-6} * (V_{\text{gas}}/22.41)$$

$F_{\text{river to atm mol/min}}$ = Flux of methane from river to atmosphere (mol/min)
V_{gas} = Volume of gas in the box

Equation (8)

$$F_{\text{river to atm mg/m}^2\text{day}} = (F_{\text{river to atm mol/min}}) * (1440\text{min/day}) * (16.043\text{g/mol}) * A_{\text{box}} * (1000\text{mg/g})$$

$F_{\text{river to atm mg/m}^2\text{day}}$ = Flux of methane from river to atmosphere (mg/m^{2}day)
A_{box} = Area of the water surface in box (m)

Using the basin size of the Schwentine of 457 km^2, the flux range of 0.29–59.34mg CH_4/m^{2}day determined using the gas collection boxes, and assuming that the range applied to the whole river basin, an approximate flux range of methane from the river water to the atmosphere can be generated by:

Equation (9)

$$F_{basin\ to\ atm\ kg/yr} = F_{river\ to\ atm\ mg/m^2day} * A_{basin} * 365days$$

$F_{basin\ to\ atm\ kg/yr}$ = Methane flux from basin (kg/yr)
$F_{river\ to\ atm\ mg/m^2day}$ = Methane flux from river per square meter per day (0.28mg/m^2day for minimum, 59.34mg/m^2day for maximum)
A= Area of river basin (457,000,000m^2)

The river may contribute between 48,374–9,898,209kg CH_4/year. This upper boundary is likely a significant overestimate because the measurements were taken in the daytime at the most downstream location, where the methane concentrations are probably the highest in the river. The large flux range supports that there is ebullition and diffusion happening in the river. The atmospheric flux is certainly not constant in the river. Better constraints on the magnitude of contribution ebullition and diffusion have on the atmospheric flux and the variability of the atmospheric flux downstream should be taken into consideration in future research.

7.9: River Flow Rate

The river flow rate does appear to decrease from the site at Oppendorf (‘Bridge 2’, see Figure 2) taken by the Schleswig-Holstein Agency for Coastal Defense, and the ‘Last Bridge’ site (Figure 2), where the orange flow test was performed by our research group on September 17, 2010. The flow measured at ‘Last Bridge’ (Figure 2) by tracking three oranges over a defined path downstream, averaged to approximately 3m^3/sec. During this day, the Schleswig-

Holstein Agency for Coastal Defense recorded the daily average river flow rate at Oppendorf to be 4.44m^3/sec. This suggests that there is a decrease in velocity of the river closer to the dam.

7.10: Influence of Dam Outlet on River's Methane Flux to Atmosphere

Samples were taken before and after the dam at sites 'Ladder 2' and 'Back Restaurant' (Figure 2) to determine the change in concentration over the dam. Except for one day in 2010, the concentration significantly dropped over the dam. Excluding the one day that the methane increased 50%, the concentration drop ranged from 26-57%, not taking into account dilution from fjord water at the site downstream of the dam, 'Back Restaurant' (Figure 24). In 2011, the concentration drop ranged from 23-39% (Figure 25), also not taking dilution into account. The question exists of how much of the methane concentration difference was due to dilution by low concentration Baltic waters, and how much was degassed to the atmosphere. A mixing calculation between the river water and the fjord water was used to account for dilution. The fjord water from the Baltic Sea was assumed to have a salinity of 35 and an average methane concentration of 4nM, based on Schmale et al. 2010. A salinity of 6.5 was measured at the 'Back Restaurant' sample site (Figure 2). A dilution of 19% was found through the following:

Equation (10)

$$(35\text{PSU})x + (0\text{PSU})y = 6.5\text{PSU}$$

$$x = 0.19$$

x = fraction of fjord water
y = fraction of river water

19% dilution of fjord water was used to calculate the amount of methane degassing at the dam. The concentration of methane entering the atmosphere at the dam was found by calculating the concentration of methane expected to be entering the river if dilution was the only process causing the drop in concentration between 'Ladder 2' and 'Back Restaurant.' The difference between this concentration, and the actual concentration at 'Ladder 2', is the concentration of methane leaving the water due to enhanced equilibration with the atmosphere. Equation (11) calculates the predicted concentration before the dam (at 'Ladder 2'), taking to account the dilution in the water after the dam, if no methane was lost at the dam outlet. Equation (12) is the difference between the measured and predicted value, which represents the concentration lost to the atmosphere at the dam outlet.

Equation (11)

$$(x)[CH_4]_{fjord} + (y)[CH_4]_{L2\ pred} = (1)[CH4]_{BR}$$

x = fraction of fjord water
y = fraction of river water
$[CH_4]_{fjord}$ = Methane concentration in fjord
$[CH_4]_{L2\ pred}$ = Methane concentration predicted to come from river if no methane was lost at dam outlet
$[CH_4]_{BR}$ = Methane concentration measured at 'Back Restaurant'

Equation (12)

$$[CH_4]_{outlet\ to\ atm} = [CH_4]_{L2\ meas} - [CH_4]_{L2\ pred}$$

$[CH_4]_{outlet\ to\ atm}$ = Methane concentration entering atmosphere at dam outlet (nM)
$[CH_4]_{L2\ meas}$ = Methane concentration measured at 'Ladder 2'
$[CH_4]_{L2\ pred}$ = Methane concentration predicted to come from river if no methane was lost at dam outlet

Accounting for dilution and assuming the degassing was the only sink of methane between the sample sites before and after the dam (a distance of approximately 50m) a significant flux of methane to the atmosphere was created. This flux was created by rapid mixing and depressurization enhancing the equilibration of the water with the atmosphere. The concentration lost to the atmosphere was calculated using the flow data from the orange methane, correcting for dilution, the assumption that no oxidation occurred before and after the dam, and the assumption that the methane difference remained constant over a 24 hour period. This flux to the atmosphere ranged from 0.291-1.09kg CH_4/day, or 106-398 kg CH_4/year as calculated by the following equation:

Equation (13)

$$F_{outlet\ to\ atm\ kg/day} = [CH_4]_{outlet\ to\ atm} * 10^{-9} * 16.043 g/mol * Flow\ (l/s) * 86{,}400 s * 1kg/1000g$$

$F_{outlet\ to\ atm\ kg/day=}$ Flux of methane from the river water at the dam outlet to the atmosphere
$[CH_4]_{outlet\ to\ atm}$ = Methane concentration entering atmosphere at dam outlet (nM)
Flow = Flow rate of river (l/s)

A more accurate flux would take into account that the concentrations in the water vary throughout the day. In the 22 hour methane survey, it was found that the lowest concentration measured at ‘Ladder 2’ was 73% of the highest concentration measured during the day. In addition, the Back Restaurant concentration was an average of 68% lower than the Ladder 2 concentration. To take into account the evening (low) concentrations in the diurnal cycle, a daily methane flux to the atmosphere at the dam can be calculated using 12hrs of a predicted low concentration at ‘Ladder 2’ (73% of the measured concentration) and 12 hours of the measured concentration during the day at ‘Ladder 2’. The theoretical low ‘Ladder 2’ concentration during the 22 hour survey was 73% of the concentration measured at ‘Ladder 2’ during the daytime sampling. The measured ‘Back Restaurant’ concentration has been an average of 68% lower than the measured ‘Ladder 2’ concentration during the daytime sampling. Therefore, the theoretical evening (low) ‘Back Restaurant’ concentration was 68% of the theoretical low ‘Ladder 2’ concentration to take into account degassing at the dam. These theoretical evening (low) ‘Back Restaurant’ and ‘Ladder 2’ concentrations were plugged into equations (11) and (12) to obtain the evening (low) methane concentration entering the atmosphere at the dam outlet. Equation (14) calculates the predicted ‘Ladder 2’ concentration during the evening (low). Equation (15) calculates the difference between the evening (low) predicted ‘Ladder 2’ concentration and the theoretical evening ‘Ladder 2’ concentration.

Equation (14)

$$(x)[CH_4]_{fjord} + (y)[CH_4]_{L2\ pred\ evening} = ((1)[CH_4]_{L2\ meas} * 0.73) * 0.68$$

x = fraction of fjord water
y = fraction of river water
$[CH_4]_{fjord}$ = Methane concentration in fjord (4nM)
$[CH_4]_{L2\ pred\ evening}$ = Methane concentration predicted to come from river if no methane was lost at dam outlet (nM)
$[CH_4]_{L2\ meas}$ = Methane concentration measured at 'Ladder 2' (nM)

Equation (15)

$$[CH_4]_{outlet\ to\ atm\ evening} = ([CH_4]_{L2\ meas} * 0.73) - [CH_4]_{L2\ pred\ evening}$$

$[CH_4]_{outlet\ to\ atm}$ = Methane concentration entering atmosphere at dam outlet (nM)
$[CH_4]_{L2\ meas}$ = Methane concentration measured at 'Ladder 2' (nM)
$[CH_4]_{L2\ pred}$ = Methane concentration predicted to come from river if no methane was lost at dam outlet (nM)

Using 12 hours of the daytime (high) concentration calculated in equation (12), 12 hours of the evening (low) concentration calculated in equation (15), and a river flow rate of $3m^3/s$, the diurnal atmospheric flux as a result of dam aeration is calculated to be 0.37-0.81 kg CH_4/day. Over one year, this is approximately 135-296 kg CH_4/year using the equations below. Equation (16) calculates the flux of methane from the dam, and is used with daytime concentration values and evening concentration values separately. Equation (17) calculates total flux of methane in kg/day from the river outlet to the atmosphere.

Equation (16)

$$F_{\text{outlet to atm kg/12hrs}} = [CH_4]_{\text{outlet to atm}} * 10^{-9} * 16.043\text{g/mol} * \text{Flow (l/s)} * 43{,}200\text{s} * 1\text{kg/1000g}$$

$F_{\text{outlet to atm kg/12hrs}}$ = Flux of methane from the river water at the dam outlet to the atmosphere in ½ day (kg/12hrs)
$[CH_4]_{\text{outlet to atm}}$ = Methane concentration entering atmosphere at dam outlet (nM)
Flow = Flow rate of river (l/s)

Equation (17)

$$F_{\text{outlet to atm kg/day}} = F_{\text{evening outlet to atm kg/12hrs}} + F_{\text{daytime outlet to atm kg/12hrs}}$$

$F_{\text{outlet to atm kg/day}}$ = Total methane flux from the river at the dam outlet to the atmosphere per day (kg/day)
$F_{\text{evening outlet to atm kg/12hrs}}$ = Evening (low) Flux of methane from the river water at the dam outlet to the atmosphere in ½ day (kg/12hrs)
$F_{\text{daytime outlet to atm kg/12hrs}}$ = Daytime (high) Flux of methane from the river water at the dam outlet to the atmosphere in ½ day (kg/12hrs)

7.11: Methane Flux from River to Fjord

Using the methane concentrations measured just after the dam at the 'Back Restaurant' sample site and accounting for fjord dilution, the methane flux to the fjord from the river can be estimated. The evening (low) concentration at 'Back Restaurant' in the diurnal cycle was estimated the same way as in the above calculation, assumed to be 68% of the estimated evening (low) concentration at 'Ladder 2'. The estimated evening (low) concentration at 'Ladder 2' was assumed to be 73% of the 'Ladder 2' concentration measured in the daytime. The measured concentration in the early afternoon was used in the daily flux calculation for 12 hours of the day, and the low concentration estimate was used for the remaining 12 hours. The orange test flow result of $3m^3/s$ was

used for the flux calculation. The contribution of methane from the river to the fjord ranged from 2.11-4.52kg CH_4/day. This totals to 770-1650kg CH_4/year. The calculations for this flux follow. Equation (18) calculates the concentration of methane entering the fjord in the daytime. Equation (19) calculates the concentration of methane entering the fjord in the evening. Equation (20) separately calculates the flux of methane entering the fjord from the river in the daytime and evening. Equation (21) calculates the total flux of methane entering the fjord from the river per day.

Equation (18)

$$[CH_4]_{\text{daytime entering fjord}} = [CH_4]_{\text{L2 meas}} - ([CH_4]_{\text{L2 meas}} * \%_{\text{lost to atm}})$$

$[CH_4]_{\text{daytime entering fjord}}$ = Methane concentration entering the fjord in the daytime
$[CH_4]_{\text{L2 meas}}$ = Methane concentration measured at 'Ladder 2' (nM)
$\%_{\text{lost to atm}} = [CH_4]_{\text{outlet to atm}} / [CH_4]_{\text{L2 meas}}$

Equation (19)

$$[CH_4]_{\text{evening entering fjord}} = ([CH_4]_{\text{L2 meas}} * 0.73) - (([CH_4]_{\text{L2 meas}} * 0.73) * \%_{\text{lost to atm}})$$

$[CH_4]_{\text{evening entering fjord}}$ = Methane concentration entering the fjord in the evening
$[CH_4]_{\text{L2 meas}}$ = Methane concentration measured at 'Ladder 2' (nM)
$\%_{\text{lost to atm}} = [CH_4]_{\text{outlet to atm}} / [CH_4]_{\text{L2 meas}}$

Equation (20)

$$F_{\text{entering fjord kg/12hrs}} = [CH_4]_{\text{entering fjord}} * 10\text{-}9 * \text{Flow (l/s)} * 16.043\text{g/mol} * 43{,}200\text{s} * 1\text{kg}/1000\text{g}$$

$F_{\text{entering fjord kg/12hrs}}$ = Flux of methane from river into fjord in ½ day (kg/12hrs) in daytime or evening
$[CH_4]_{\text{entering fjord}}$ = Methane concentration entering the fjord in the daytime or evening

Flow = Flow of river (l/s)

Equation (21)

$$F_{\text{entering fjord kg/day}} = F_{\text{evening entering fjord kg/12hrs}} + F_{\text{daytime entering fjord kg/12hrs}}$$

$F_{\text{evening entering fjord kg/12hrs}}$ = Flux of methane from river into fjord in evening
$F_{\text{daytime entering fjord kg/12hrs}}$ = Flux of methane from river into fjord in daytime

7.12: Methane in Brackish Discharge Zone after Dam

Water samples taken in the fjord on July 15, 2011 showed that methane concentration gradually decreased away from the dam in the surface waters. In the deeper waters, methane gradually decreased until Site 3, where it began to increase (Figure 26). All the concentrations in the deeper waters were significantly lower than in the surface waters except for at the site farthest from the dam. The dissolved oxygen concentration displayed an opposite spatial trend with methane in the surface as well as the deep waters (Figure 27 and Figure 28). In the surface waters, dissolved oxygen negatively correlated with methane with an r^2=0.7253 (Figure 29). In the deep waters, dissolved oxygen negatively correlated more strongly with methane with an r^2=0.8748 (Figure 29). It is not certain why this occurred. Salinity steadily increased in the surface waters away from the dam (Figure 30). Salinity also increased in the deep waters except at Site 5, where a slight freshening of 10.3PSU (from 27.3PSU at Site 4 to 16.8PSU at Site 5) occurred (Figure 30). Salinity correlated very well with methane in the surface and deep water, having an r^2=0.9777 and r^2=0.9282, respectively.

The three cores taken on July 15, 2011 showed methane concentrations increased with depth (Site 1 core, Figure 31; Site 2 and 4 cores, Figure 32). Site Methane reached higher and higher concentrations in the sites farther from the dam. The peak in methane production was not near the surface of the cores, suggesting a sulfate reduction zone between the zone of methanogenesis and the sediment water interface.

CHAPTER 8: DISCUSSION

8.1: Spatial Variability of Methane in the River

The methane concentration increased an average of 200% in 2011 between the most upstream site, 'Birdhouse Clearing', and the most downstream site, 'Ladder 2'. There are two possible explanations for the methane concentration increase downstream toward the dam. First, methane concentration increased downstream because of accumulation of methane in the water column from the sediment pore water. Second, methane from runoff discharge accumulated downstream.

In the first scenario, methane production in the sediment and contribution to the water column exceeds the sinks of methane (oxidation and diffusion to the atmosphere). This theory is not explored further in this study because core data is not available to generate a methane flux of diffusion and ebullition from the sediment pore water to the water column. In addition, oxidation rates and comprehensive diffusion rates to the atmosphere are not available to generate an accurate model.

The second scenario involves the increase in the runoff source of methane to the river downstream. This theory was introduced by de Angelis and Lilley, 1987, who discussed that a river's methane concentration should increase downstream as a result of increased drainage area and the accumulation of methane from tributaries and the upstream waters. It is a distinct possibility that this is the case in the Schwentine. Numerous drainage channels empty into the river. The one channel sampled in this study, site 'Drainage Channel', had

methane concentrations one to two orders of magnitude higher than the river water. These drainage channels have the potential to be significant sources of methane to the river. The accumulation of methane from these channels appeared to be the most likely dominant factor affecting the spatial variability downstream.

It is also possible that the dam influenced the production of methane in the sediment. The dam caused the velocity of the river to decrease. The distance upstream that the dam affected the velocity is currently not known due to inadequate flow measurements spatially upstream. However, we know the river is slowed downstream by the flow measurements taken by our research group and the Schleswig-Holstein Agency for Coastal Defense. When the velocity is decreased, more of the suspended organic load may settle and accumulate in the sediment. This is a theory, as the data for sediment accumulation in the river cores is not currently available. If there is higher deposition of organic matter to the sediment, more oxygen is utilized in aerobic decomposition. When all oxygen is consumed, anaerobic decomposition occurs and methane is produced via methanogenesis. The more organic material deposited, the faster oxygen is consumed with depth in the sediment. This may allow methanogenesis to occur close to the sediment-water interface. If this is the case, methane may diffuse into the water column from the sediment pore water. If methanogenesis increases closer to the dam, the methane concentration in the river water may increase downstream. However, since the increase in river methane

concentration downstream starts at least 3km upstream from the dam, the dam is not likely a dominant factor affecting the increase of methane downstream.

All of the above likely influence the spatial concentration variability of methane in the river system. However, runoff was most likely the dominant factor affecting the increase in river methane concentration downstream. In any case, the river concentrations are supersaturated with respect to the atmosphere and will generate an atmospheric methane flux from the river that should not be disregarded.

8.2: Diurnal Variability of Methane in River

There is a strong diurnal trend in methane concentration, with the highest methane concentration in the daytime and the lowest in the nighttime (Figure 9). The diurnal trend in methane concentration closely follows the diurnal trend in air temperature and solar irradiance over the 22 hour methane sampling period (Figure 10). It has been shown that humidity and air-leaf temperature, ultimately controlled by diurnal changes in solar irradiation, influences the internal pressure and gas transport of methane through plants ((Dacey, 1981 a and b; Dacey and Klug, 1982; Grosse and Mevi-Schutz, 1987; Armstrong and Armstrong, 1990; Brix et al. 1992; Brix et al. 1993; Chanton and Whiting, 1996; Long et al. 2009). Although little research has been done on the effect plant ventilation processes have on the methane concentration in the water column, it has been shown that plant gas transport processes including convective ventilation and molecular diffusion significantly affect atmospheric methane emissions (Sebacher et al.

1985; Chanton et al. 1993). It is possible that diurnal cycles in plant ventilation gas transport modes were causing the diurnal trend in river water methane in this study. However, analysis of the plant types in the river and isotopic data to reveal their gas transport behavior is needed to reach any conclusion. The reason for this diurnal cycle is not explored further in this thesis.

There was a small methane peak at ‘Ladder 2’ around midnight that has no obvious explanation. It is possible that this evening peak was due to a change in wind speed or a change in the river flow rate. It appears in Figure 33 that the evening peak in methane concentration at ‘Ladder 2’ coincided with a weakening of the winds. Weak winds may have led to higher methane concentrations in two ways. First, the turbulence and piston velocity (defined in section 8.3: Temporal Variability of Methane in River) was reduced, reducing the exchange across the water-atmosphere interface. Second, reduced turbulence made the system less well mixed. Both of these scenarios reduce the flux to the atmosphere and may have allowed methane to accumulate in the water.

A change in river flow rate in the evening may have affected methane concentration variability during the 22 hour survey. Figure 34 shows that the water samples taken at 18:35 and 20:15 corresponded with peaks in river flow rate. Both these samples formed a trough in the diurnal trend, having concentrations 78-117nM less than the samples taken earlier in the day at 13:06 and 15:20. Although a record of the dam opening is not available at this time, it is possible that the dam was opened later in the evening. This would have increased flow rate, and drawn the lower methane concentration river water

further downstream. This would have resulted in an anthropogenically induced trough within the natural diurnal cycle of methane in the river. If this trough was not present, the diurnal cycle of methane would gradually decrease in the evening and increase during the daytime. Excluding the trough created by samples taken at 18:35 and 20:15 from the diurnal cycle, we saw that the evening peak disappeared (Figure 35). To confirm that the dam was opened in the evening, a record of the dam adjustments should be pursued in the future. To confirm that lower concentration water was pushed downstream during this peak in flow rate, a spatial transect should be performed periodically throughout the evening. However, it appears that dam operations may be a dominant factor affecting the overall temporal variability in methane concentrations downstream. The opening and closing of the dam may have implications on the maximum and minimum concentration potential of the river, the diffusive flux to the atmosphere resulting from these concentrations, the amount of methane degassed to the atmosphere at the dam, and the amount of methane released into the fjord.

A shift in wind direction may have had an influence on the diurnal variability of methane in the river. Wind direction data taken by the IFM-Geomar Weather Station during the 22-hour survey does show the shift from onshore winds during the daytime to offshore winds during the evening (Figure 36). This change in wind direction may have had implications on the methane concentration, however presence or magnitude of the effect is not known at this time.

It should be mentioned that a large touring boat that routinely traveled up and down stream may have had an influence on the methane concentration in the water. It was seen that as the boat passed through the water, ebullition was enhanced. Although this may have had an influence on the methane concentration, the daytime methane increase seen during the 22 hour survey did not match up with the time the boat tours began. However, when the boat tours stopped for the day (around 5pm), it is plausible that the water became less well mixed. Although the boating may have had an effect on the river mixing and surface water methane concentration, the extent of this effect is not known at this time.

8.3: Temporal Variability of Methane in River

Very little correlation was seen between methane concentration in the surface river water and wind speed. It was thought there might be a correlation with wind speed, as it affects the surface turbulence in the water. This increases the piston velocity (Stumm and Morgan, 1996), a component of the flux defined by the diffusion divided by thickness of a stagnant boundary layer.

Equation (22)

$$F = (1/(V_w^{-1} + V_a^{-1} * H)) * (c_w - c_a * H)$$

F = Flux
$V_w = D_w/z_w$
$V_a = D_a/z_a$
D_w = diffusion coefficient in water
D_a = diffusion coefficient in air

z = thickness of stagnant water layer
z = thickness of stagnant air layer
$H = c_{w/a}/c_{a/w}$
$c_{w/a}$ = concentration in water film at air-water interface
$c_{a/w}$ = concentration in air film at air-water interface
c_w = concentration in well mixed water
c_a = concentration in well mixed air

High wind speeds increase turbulence, which decreases the thickness of the stagnant boundary (z), which increases the piston velocity (V) and diffusion coefficient (D), which then increases the flux to the atmosphere (F) as defined by Fick's first law of diffusion:

Equation (23)

$$F = -D(\delta c/\delta z)$$

F= diffusive flux
D= diffusion coefficient
c= concentration
z= thickness of layer

There was no correlation when plotting methane concentration with wind speed, having an r^2=0.041 (Figure 13). However, the methane data set generated in this study may not be large enough to see a correlation.

In 2010, there did appear to be a correlation with water temperature (Figure 12). We might expect to see this because a decrease in water temperature increases the solubility of methane. However, it is unlikely that this difference would be seen with such small variability in water temperature (16.6–

21.3℃) compared to the large variability seen in methane concentration (386 – 1513nM). The largest difference in methane concentration between sample days at ‘Ladder 2’ was on July 14 and August 2, 2011. The difference in concentration was 546nM, with 1327 ± 47nM on July 14 and 781 ± 47nM on August 2. However, the water temperature on both days was the same at 28.5℃. For a change in temperature to lower the concentration on July 14 at ‘Ladder 2’ by 600nM, the temperature would have had to increase by 195.5℃.

When the average daily methane concentration was plotted with precipitation, a weak positive relationship was seen (Figure 14). The precipitation might have diluted the methane in the river water and caused a negative correlation with dissolved methane concentration. However, it appears that precipitation induced a uniform increase in methane concentration throughout the river, likely caused by increased runoff after a precipitation event.

The high methane concentration of the runoff and drainage channels was confirmed by measurements taken at site ‘Drainage Channel’. These channels were created by land runoff and pipes draining water from the surrounding area. As the Schwentine is partially surrounded by agricultural land, it is expected that the drainage water contains ruminant waste and nutrients from fertilized soils. This is confirmed by the elevated dissolved phosphate concentration at the ‘Drainage Channel’ site relative to the river. The high nutrient content from the runoff water stimulates productivity. Methane reaches very high concentrations in this channel, between 261 and 4719% higher than ‘Birdhouse Clearing’ methane concentrations measured in the river ~100m upstream from the channel. The

methane was delivered to the channel by the runoff water, and/or was produced in situ in the sediment in the drainage channel. This resulted in a very high concentration of methane in the channel water. The temperature, dissolved oxygen, and methane difference between the drainage channel and the river at site downstream from the channel, site ‘Flatdock’ (Figure 2), show that the channel water is not well mixed with the river water. If precipitation events force the high methane concentration water in these channels into the river, the drainage from this channel and others that are present in the Schwentine was likely responsible for the temporal variability of methane in the river seen between sample days.

Our data show that peaks in methane concentration coincided with peaks in river flow rate, which were preceded by peaks in precipitation. The overall methane concentration variability seen in the river appeared to be dominated by runoff. When a precipitation event occurred, the drainage from the land to the river increased. This increased the flow rate, as shown in Figure 16. This suggests that drainage was a dominant factor controlling temporal methane variability in the river.

Drainage runoff, as well as the opening and closing of the dam, appeared to be the dominant factors affecting the temporal variability of methane in the river. These factors should be taken into account when estimating riverine methane concentration and the methane contribution of rivers to the atmosphere and coastal waters. The presence of drainage channels, the volume and

periodicity of runoff, and the presence and operations of a dam should be considered when determining the methane variability in a river system.

8.4: Flux of Methane to Atmosphere from River before Dam

The atmospheric flux measured in 2011 using the collection boxes between sites 'Ladder 2' and 'Last Bridge' (Figure 23) generated daily emissions significantly lower than the emission data from the Florida canal reported by Zimmerman (1977). Emissions from the Schwentine ranged from 0.29-59.34mg CH_4/m^2day, where the Florida canal emitted an average 140mg CH_4/m^2day. This is likely the result of climate difference between the two study sites. Warmer temperatures in Florida are likely to stimulate more methane production as a result of higher productivity in the water column. However, Del Sontro et al. 2010 found methane emissions from Lake Wohlen, a hydropower reservoir in Switzerland, to have emissions of >150mg CH_4/day. Ebullition was the dominant emission pathway of methane from the river to the atmosphere. Therefore, the temperate water systems can have high methane emissions comparable to lower latitude rivers. Although the emission estimates in the Schwentine are much lower, ebullition was not fully accounted for even though it was visually observed. Future studies should attempt to discriminate between the diffusive and ebullition flux to generate more accurate values. In addition, further studies should be done to understand the variability of atmospheric flux from rivers in temperate climates, as Cicerone and Shetter (1981), Harriss and Sebacher (1981), and de Angelis

and Lilley (1987) discussed that there is high variability among data sets from similar regions as well as limited data coverage of river emissions.

8.5: Flux of Methane from River to Atmosphere at Dam Outlet

The dam appeared to have a significant influence on the methane concentration in the river outflow. The dam outlet vigorously mixed the water, and enhanced the equilibration of the water with the atmosphere. This might make dams a small but notable greenhouse gas budget concern since they form a microsystem that facilitates an unnaturally high flux of methane to the atmosphere. 19% dilution by low methane concentration fjord water is taken into account in our concentration measurement after the dam. The maximum salinity measured (6.7PSU) was used in the mixing model to calculate the minimum atmospheric flux at the dam. The maximum atmospheric flux is calculated assuming no diurnal variability of methane. This provides an upper end atmospheric flux range of 106-398kg/year of CH_4. Taking into account dilution and diurnal variability, the atmospheric flux at the dam ranges from 135-296kg CH_4/year into the atmosphere. This is likely to still be an overestimate, as measurements were taken in the summer and seasonal variations are not considered.

Another variable that might alter these estimates is oxidation of methane over the dam outlet. However, the time it takes for a parcel of water to get from the site before the dam (site ‘Ladder 2’) to after the dam (site ‘Back Restaurant’)

is on the order of seconds. Therefore, it is unlikely that methane oxidation had a significant effect.

Although the drop in concentration over the dam in the Schwentine was lower than the concentration drops measured by Galy-Lacaux et al. 1997 and Abril et al. 2005, the flux to the atmosphere as a result of aeration at the dam is not negligible. In order to accurately constrain the contribution of methane from temperate fresh water bodies, the flux resulting from degassing at dams should be further investigated and quantified at additional sites.

8.6: Methane Flux from River to Fjord

Despite the release of methane at the dam, a significant amount of methane reached the coastal fjord waters. The methane concentrations from the Schwentine entering the fjord fell in the middle of the ranges reported in Potomac River, Chesapeake Bay, and York River (Lamontagne et al. 1973), Sepik River (Wilkniss et al. 1978), Mississippi River (Swinnerton and Lamontagne, 1974), Yaquina River (Butler et al. 1987 and de Angelis and Lilley, 1987), Amazon River (Richey et al. 1988), the Alsea River, Siletz River, McKenzie River, Willamette River (de Angelis and Lilley, 1987), and the predicted values for the Rhine and Western Scheldt Rivers (Scranton and McShane, 1991). A summary table of the river methane concentrations provided by Scranton and McShane, 1991, including the Schwentine's results, is shown in Table 2. Scranton and McShane, 1991, reported that although rivers are unlikely to be significant sources of methane to the atmosphere, they do have the potential to be important sources

of methane to the coastal waters. The Schwentine river water, after the dam aeration and dilution, ranged from 429-1327 ± 49nM in 2011. An estimated 2.11–4.52kg CH_4/day is released in the fjord from the water each day or 770–1650kg CH_4/year. This calculation is provided in subchapter 7.11: Methane Flux from River to Fjord.

8.7: Water Column and Pore Water Chemistry in Brackish Discharge Zone

Analysis of methane and salinity concentrations in the fjord water column and methane in sediment pore waters provided insight into the dominant source of methane to the coastal waters. The salinity data showed river water entered the fjord in a hypopycnal flow because the surface water was much fresher than the deep water at Sites 1-4. The difference in salinity between the surface and deep waters at Site 1 (closest to the dam) was approximately 3PSU, whereas the other sites further from the dam and with deeper water columns varied between 5-9PSU (Figure 37). This was likely due to more mixing in the shallow water closer to the dam. If the river was the dominant source of methane to the coastal waters, the methane should have been higher in the surface water than in the deep water in the Brackish Discharge Zone. Figure 26 shows the methane concentrations at Sites 1-4 were higher in the surface waters. This suggests that the river was the dominant source of methane to the coastal waters near the dam.

The decrease in the surface water methane concentration away from the dam was likely the result of a combination of the following: dilution by mixing with the low methane concentration Baltic waters, oxidation of methane, and flux to the atmosphere. Dilution from the fjord waters was the most dominant process, since dissolved methane concentration negatively correlated with salinity in the surface water (r^2=0.9777) and deep water (r^2=0.9282) as shown in Figure 37. Since the saturations ratios (R) of methane in the surface water ranged from R=152 (608nM) at Site 1 to R=39 (155nM) at Site 5, it is likely that this high methane river water is contributing to the oceanic flux in this region. The methane saturation ratios did decrease away from the dam, but the water was still supersaturated with methane with respect to the atmosphere.

The deep water column methane concentration increasing at Sites 4 and 5 may be the result of increased methane productivity in the sediment. The methane concentration increased in the cores going away from the dam. Although sediment deposition rates are not known, the Schwentine may drop more of its organic load farther from the dam where these high concentrations were found in the pore waters. If the sulfate is rapidly consumed with depth in the sediment during anaerobic decomposition, the methane in the pore water below the sulfate-methane transition zone may enter the water column by ebullition or diffusion if porosity is high or methanogenesis occurs very close to the sediment water interface. However, the peak in methane production was centimeters deep in the cores. It is likely that a sulfate reduction zone resides between the zone of methanogenesis and the sediment water interface. Therefore, it is unlikely that

the sediment pore water was a dominant source of methane to the water column in this region.

CHAPTER 9: CONCLUSION

This study at the Schwentine showed that a small, dammed river can be complex with regards to its spatial and temporal variability of methane. The data provided insight into the dominant processes affecting methane concentration in a river system and its outlet. These variables are important to understand when estimating the contribution of freshwater river systems to the atmosphere and coastal waters.

The diurnal variability of methane concentration in the Schwentine was likely dominated by two processes, by fluctuations in solar irradiance affecting gas transport in aquatic plants, and by increase in flow rate caused by opening of the dam creating an additional evening low in methane concentration. Natural diurnal variability as well as opening and closing of the dam should be taken into consideration when calculating methane fluxes to the atmosphere and coastal waters.

Precipitation induced runoff was the dominant factor influencing the temporal variability between sample days. Although weather factors such as water and air temperature, wind speed, and solar irradiance may play a role in methane concentration, their role is too small to be determined in the temporal variability seen in this study. Runoff should be taken into account when determining the inputs of methane to a river system, as well as when estimating annual methane fluxes to the atmosphere and coastal waters from the river.

The spatial variability of methane in the Schwentine appeared to be dominated by the accumulation of runoff methane downstream. Since methane

concentrations were highly spatially variable, the atmospheric methane flux is likely also highly variable over the entire river. This should be taken into consideration to better constrain the methane contributions of rivers to the atmosphere in the future.

The dam provided a notable source of methane to the atmosphere. The outlet vigorously aerated the water, resulting in 5 to 25% of the methane in the water before the dam to be released to the atmosphere. This creates a 135–296kg/year source of methane to the atmosphere. The methane flux to the atmosphere from dammed rivers should be further studied and accounted for in global methane budgets.

Despite aeration at the dam, a significant amount of methane (770-1650kg CH_4/year) was released from the river into the fjord. The river appears to be the dominant source of methane to the coastal waters. Although the river supersaturated the coastal waters with methane close to the dam, the water became less supersaturated away from the dam. River discharge should be taken into account when determining the sources and sinks of methane in the ocean.

The Schwentine River is a highly complex system with many factors contributing to the spatial and temporal variability of methane in the water. Significant insight was given into the high concentrations a temperate freshwater river system can reach, and the potential impact it has on atmospheric emissions and methane in coastal waters. Insight was also given on the affect of the dam on the temporal variability of methane, degassing methane flux to the

atmosphere, and methane flux to the fjord. In addition, a better understanding was grasped on the factors influencing the spatial and temporal variability in a freshwater river system. Temperate water bodies, especially those that are dammed and influenced by agricultural runoff, have the potential to reach high and variable methane concentrations that should not be disregarded when constraining future methane budgets.

CHAPTER 10: FUTURE WORK

In order to determine the magnitude of the processes which influence methane concentration in the river, future work must be done. Further core analysis down the river transect will help better understand the contribution from the river sediment. Chemical analysis of total phosphorous and nitrogen in all of the drainage outlets into the river will better constrain the potential input of methane, as well as nutrients, to the river from runoff. Continuous surveys should be performed upstream to determine if the diurnal variability is uniform over the river. The plant life in the river should be classified and analyzed to investigate if their gas transport mechanisms are affecting the methane concentrations in the river. Further measurements of the atmospheric flux can help constrain the atmospheric emissions in the river as well as the fjord. Sampling throughout all seasons will provide a broader data set to compare with weather factors, and give a better understanding of the seasonal variability. Isotopic carbon analysis will validate our assumption that the methane in the river and fjord is all biogenic. This is more significant in determining sources of methane in coastal areas with thermogenic methane seeps. In addition, more cores should be taken in the fjord to better constrain the flux of methane from the marine sediment.

Finally, this study has shown that freshwater systems are very complex in terms of the processes affecting the spatial and temporal variability of methane. Future work should focus on attempting to classify the freshwater river systems in ways other than temperate vs. tropical to grasp a better understanding on what dominates the methane concentration potential of these systems. We have

shown runoff and the presence of a dam can have profound effects on the methane concentration. Since flow appears to have a significant effect, an attempt should be made to determine whether river average slope correlates with the average methane concentration in a river. This was not pursued in this study due to the limited data available, but should be considered in the future.

APPENDICES: Figures 1-38 and Tables 1-15

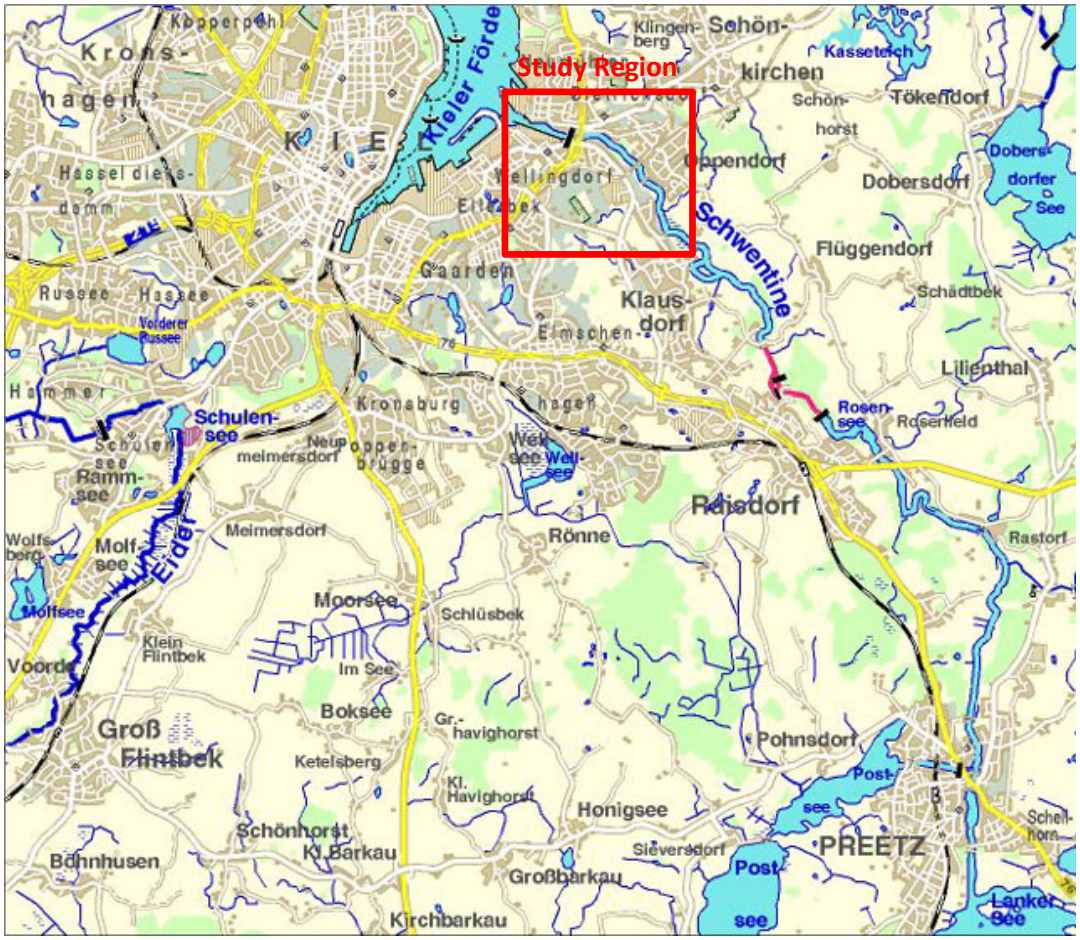

Figure 1: The Schwentine is a 70km long freshwater river in Northern Germany which empties into the Kiel Fjord (Baltic Sea). Map courtesy of Kanuland Schleswig Holstein.

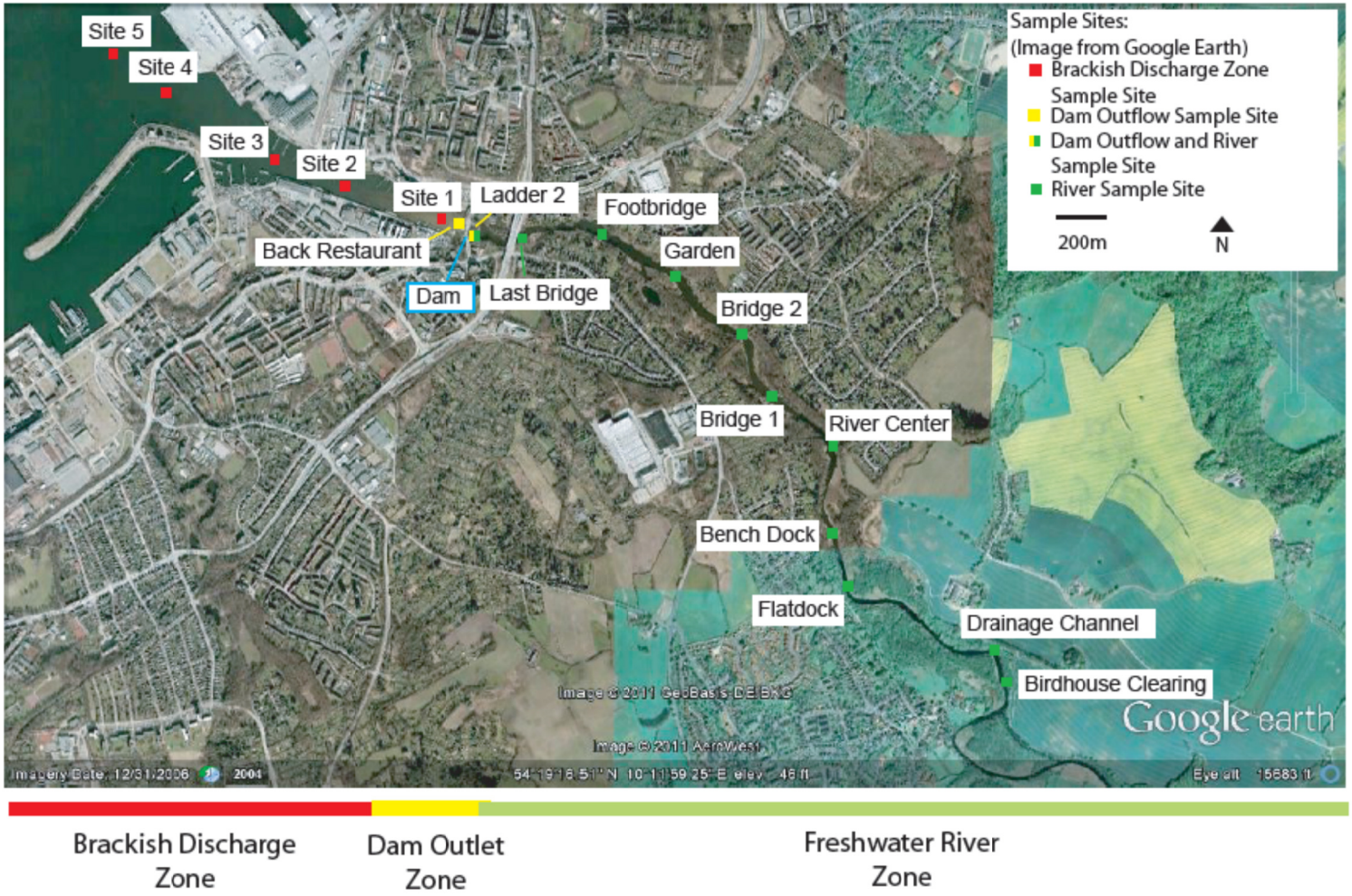

Figure 2: The sample sites in the river, dam outlet, and brackish discharge zone are shown.

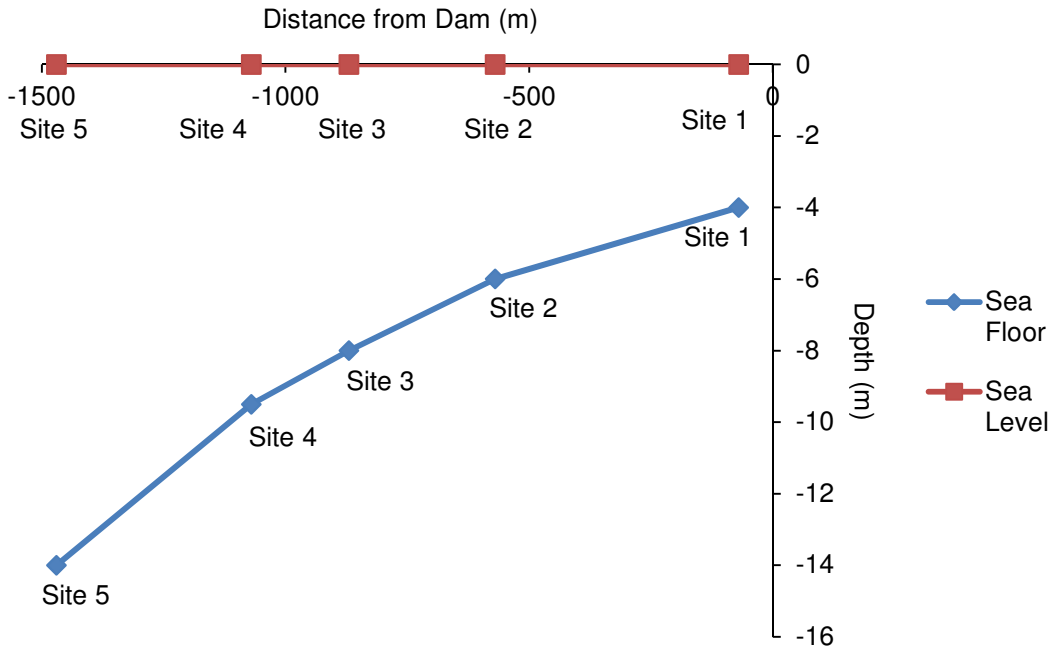

Figure 3: The depth of the sediment-water interface is shown relative to the sea surface in the Brackish Discharge Zone. The dam is represented by the origin.

Figure 4: Gas collection boxes were placed at sites A, B, and C. The dam borders the map to the left. The "Last Bridge" site borders the map to the right.

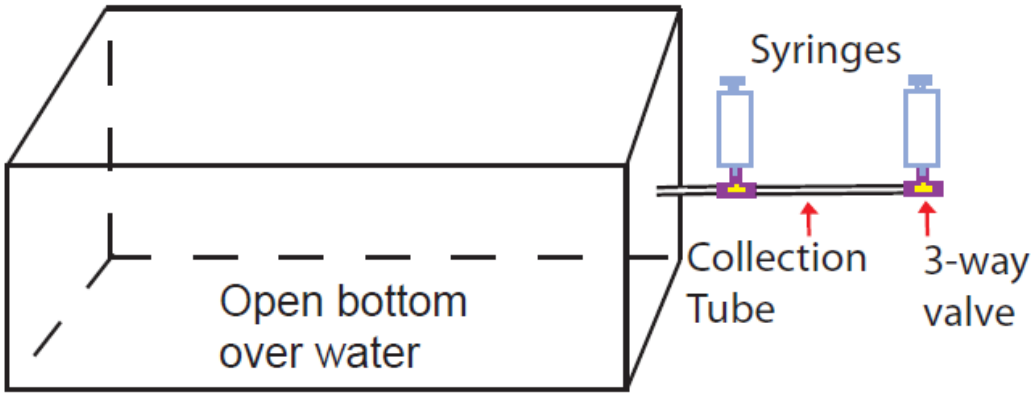

Figure 5: A schematic of the gas collection box is shown. The box open side down on the water, and is stabilized by a metal frame not shown above.

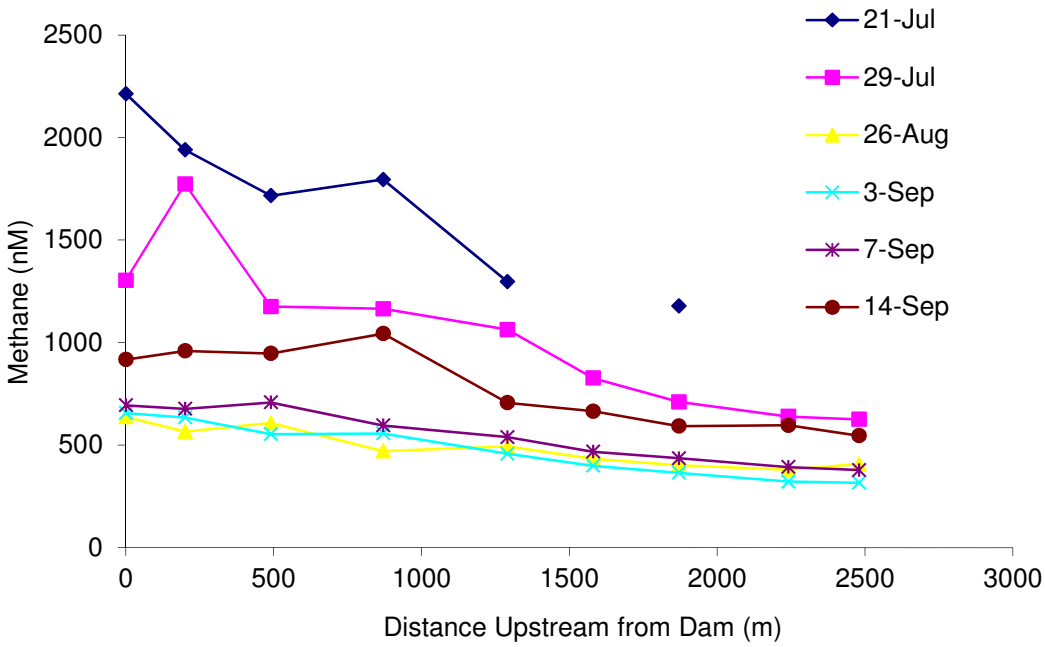

Figure 6: In 2010, the methane concentration in the river water gradually increased toward the dam. The dam and most downstream sample site in the river (site 'Ladder 2', see Figure 2) are represented by zero meters (the graph origin). The error is ± 51nM.

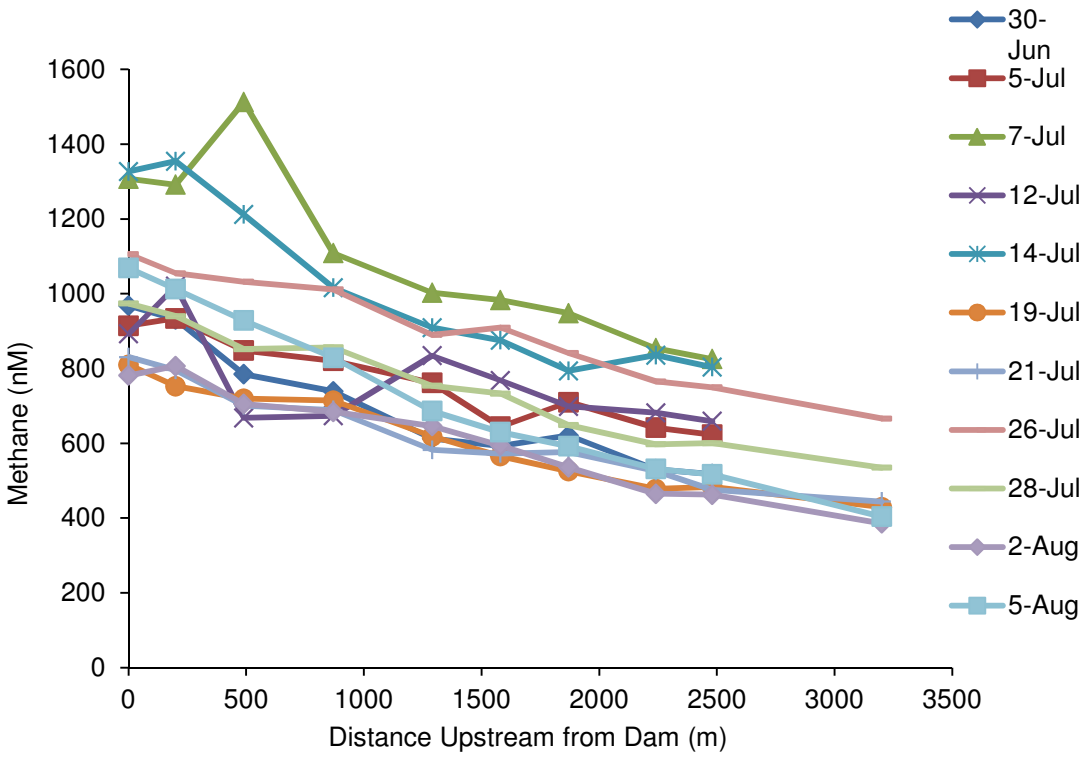

Figure 7: In 2011, the methane concentration in the river water gradually increased toward the dam. The dam and most downstream sample site in the river (site 'Ladder 2', see Figure 2) are represented by zero meters (the graph origin). The error is ± 47nM.

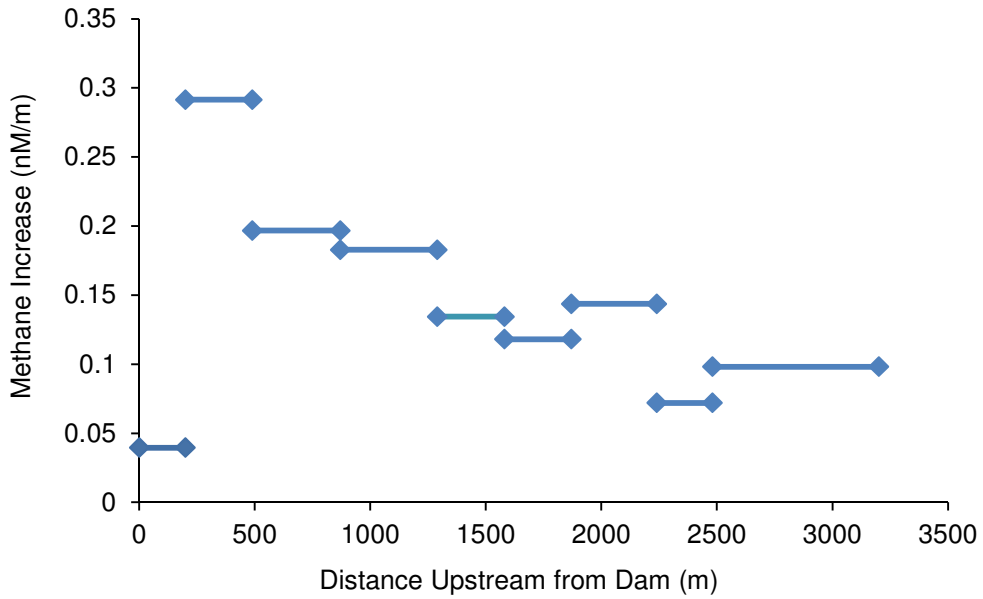

Figure 8: The increase in methane concentration per meter traveled along the river increases overall downstream. The dam and most downstream sample site in the river (site 'Ladder 2', see Figure 2) are represented by zero meters (the graph origin). The concentration increase is significantly lower near the dam due to an increase in river flow.

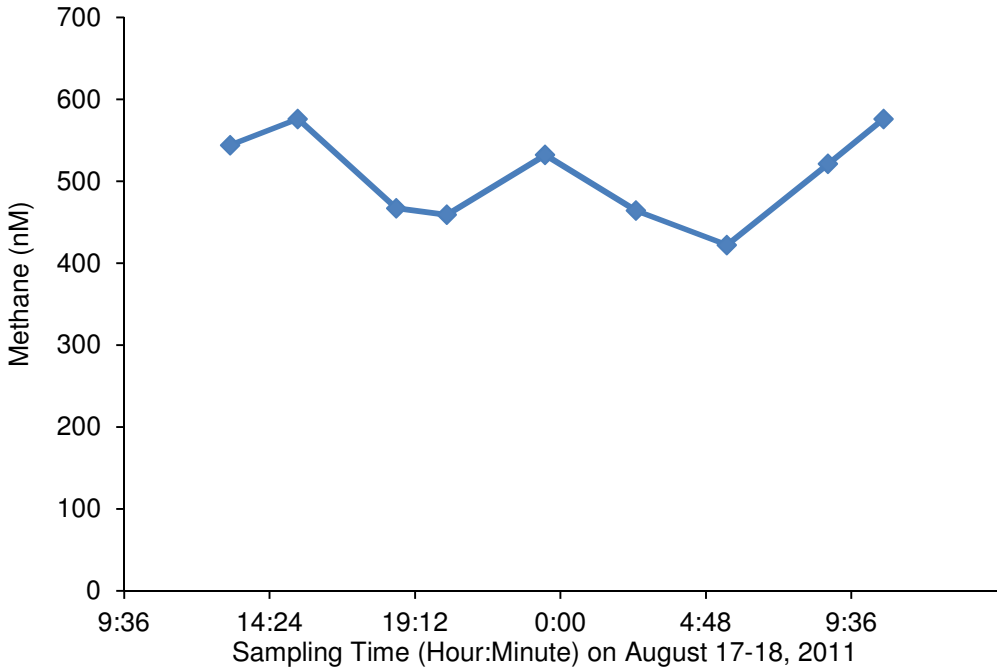

Figure 9: Samples taken over 22 hours between August 17-18, 2011 show diurnal variability in dissolved methane concentration in the river water. The error is ± 43nM.

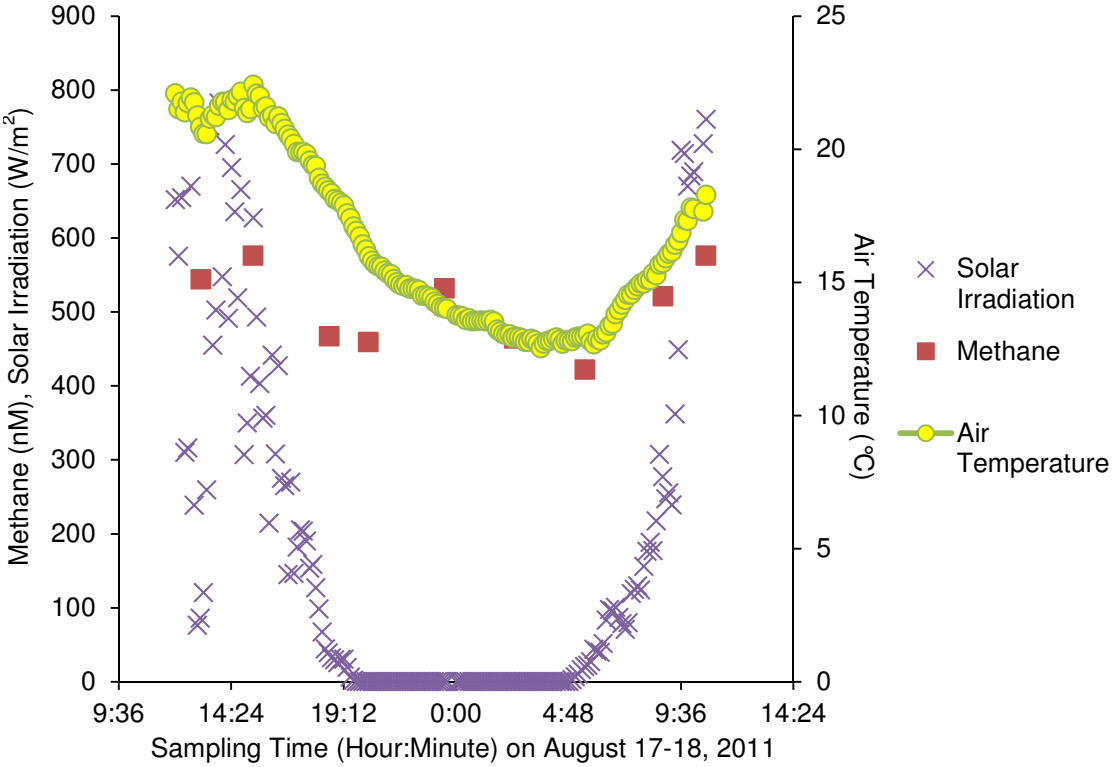

Figure 10: Samples taken over 22 hours between August 17-18, 2011 show diurnal variability in dissolved methane concentration that follows the diurnal trend in solar irradiation and air temperature. The error for methane is ± 43nM.

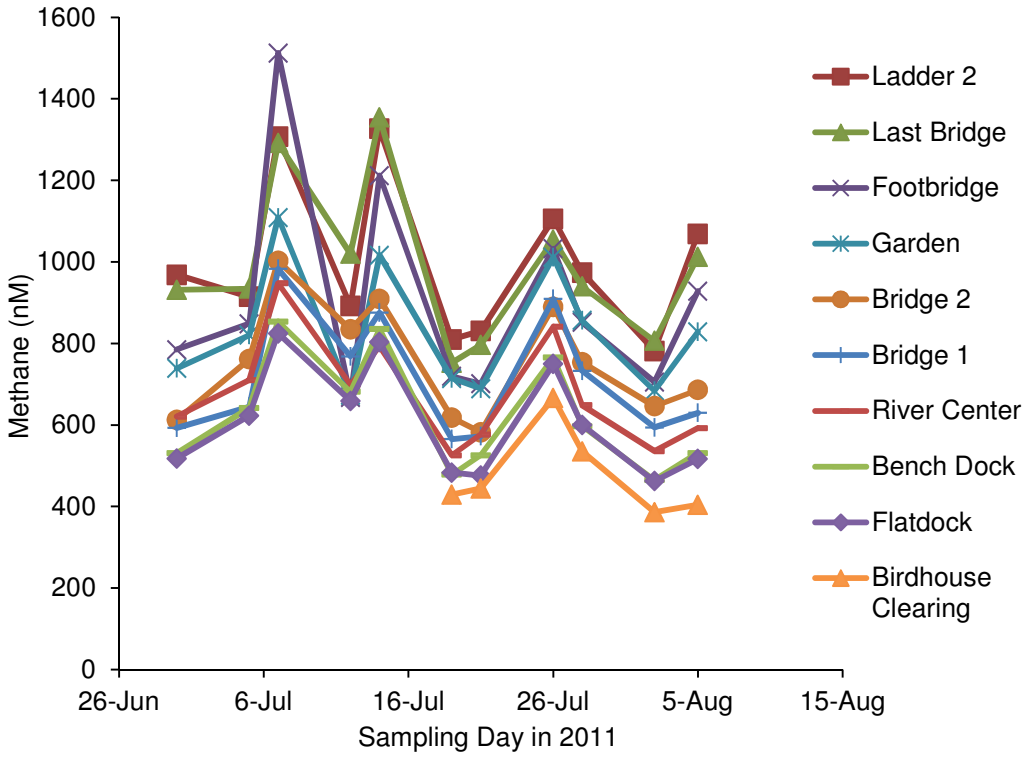

Figure 11: The dissolved methane concentration in the river water varies uniformly at all sample sites in the river between sampling days in 2011. The error is ± 43nM.

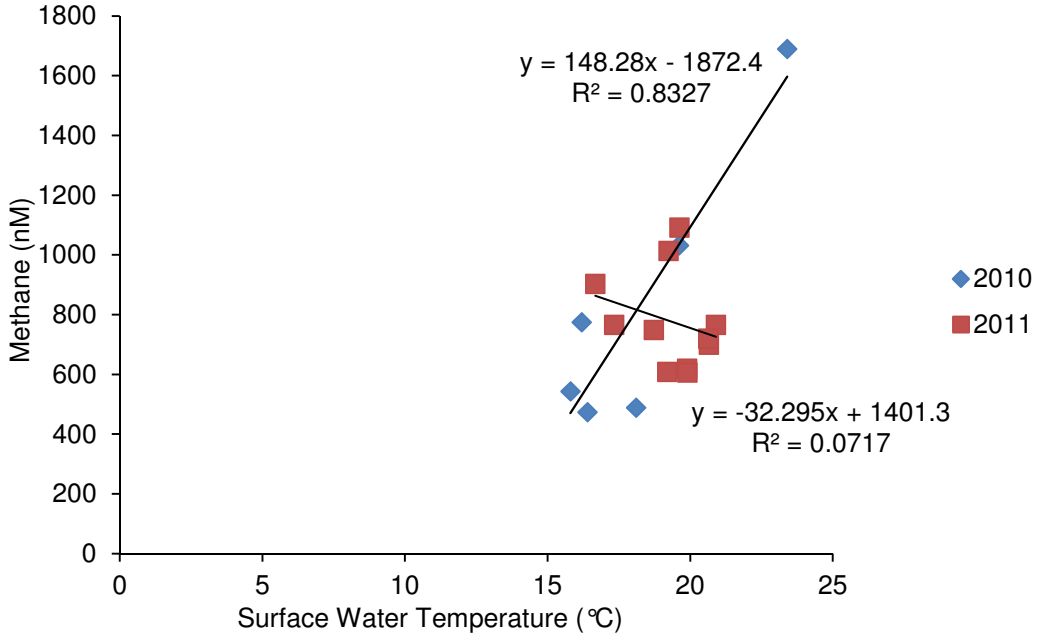

Figure 12: There appears to be a correlation between average dissolved methane in the river and the average water temperature at the surface in the samples taken in 2010.

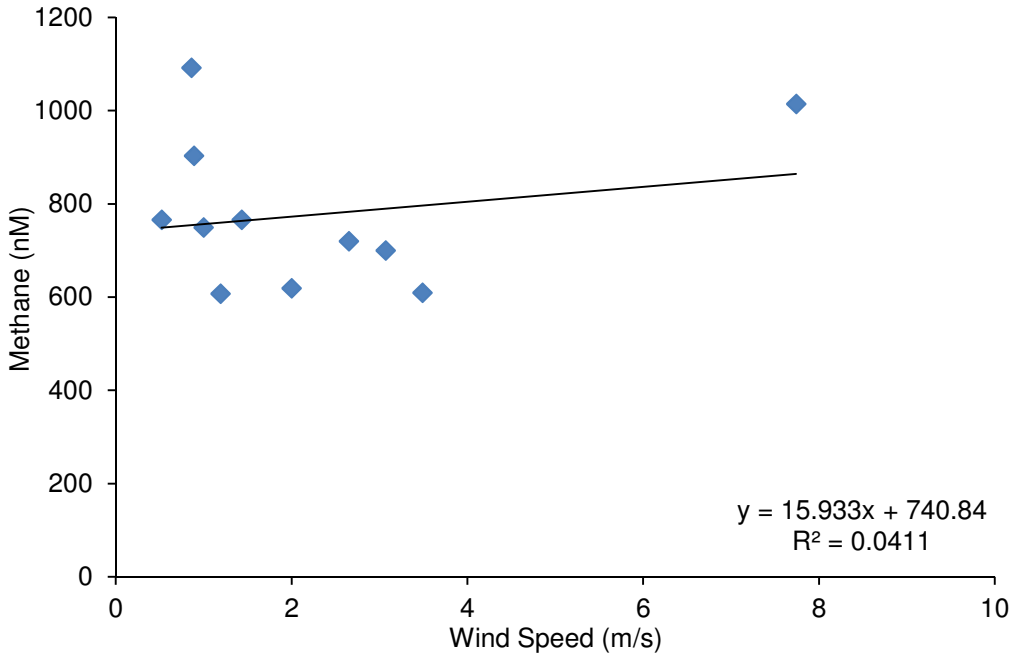

Figure 13: There appears to be no correlation between dissolved methane in the river water and the averaged wind speed from midnight to noon on the sampling days in 2011.

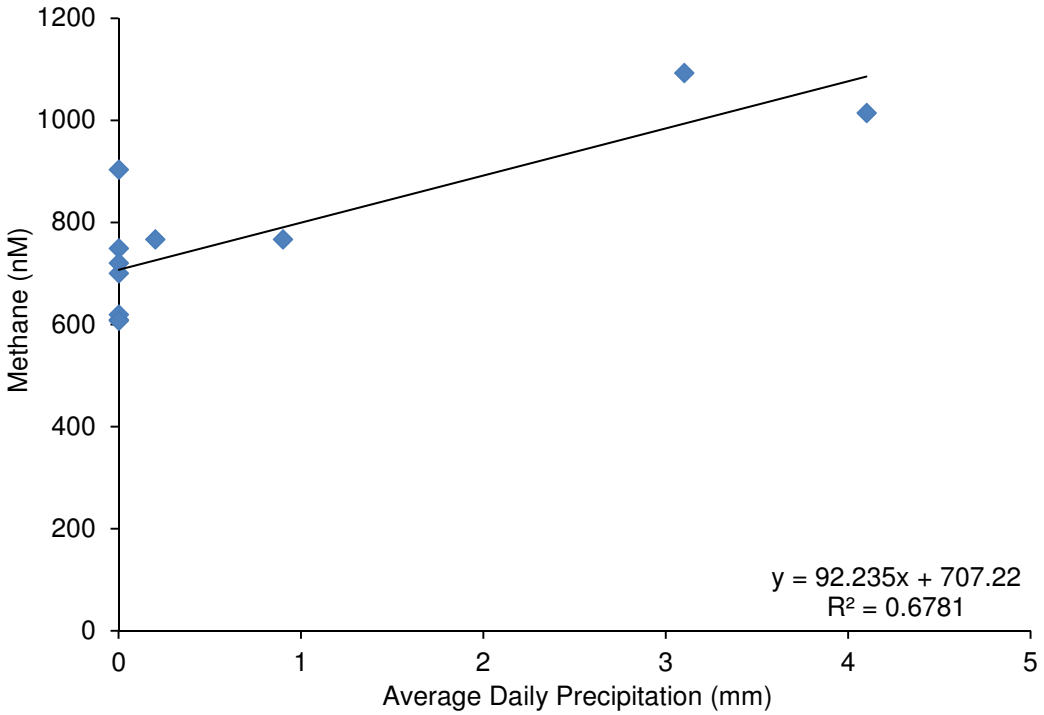

Figure 14: There appears to be a correlation between dissolved methane in the river water and average precipitation for the sample days in 2011.

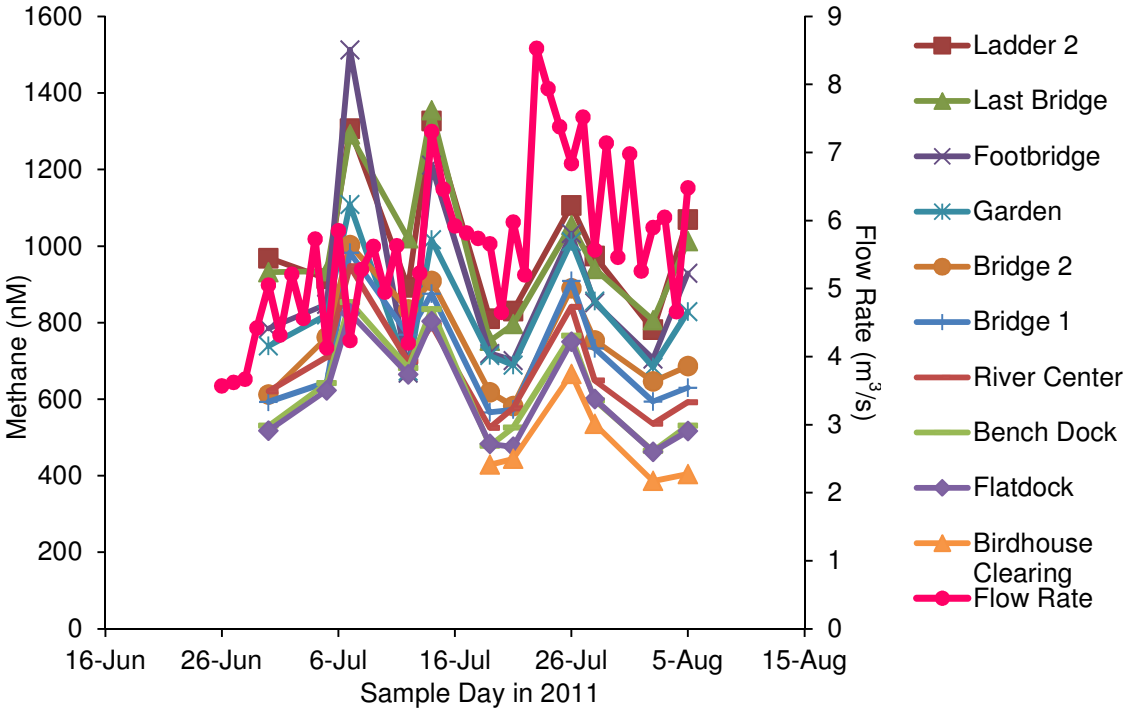

Figure 15: The largest peaks and troughs in river flow rate match the peaks and troughs in dissolved methane concentration between the sample days in 2011. Note that the flow data have a higher frequency record, and therefore not all the peaks may be matched with the lower sampling frequency dissolved methane record. The error for methane is ± 47nM.

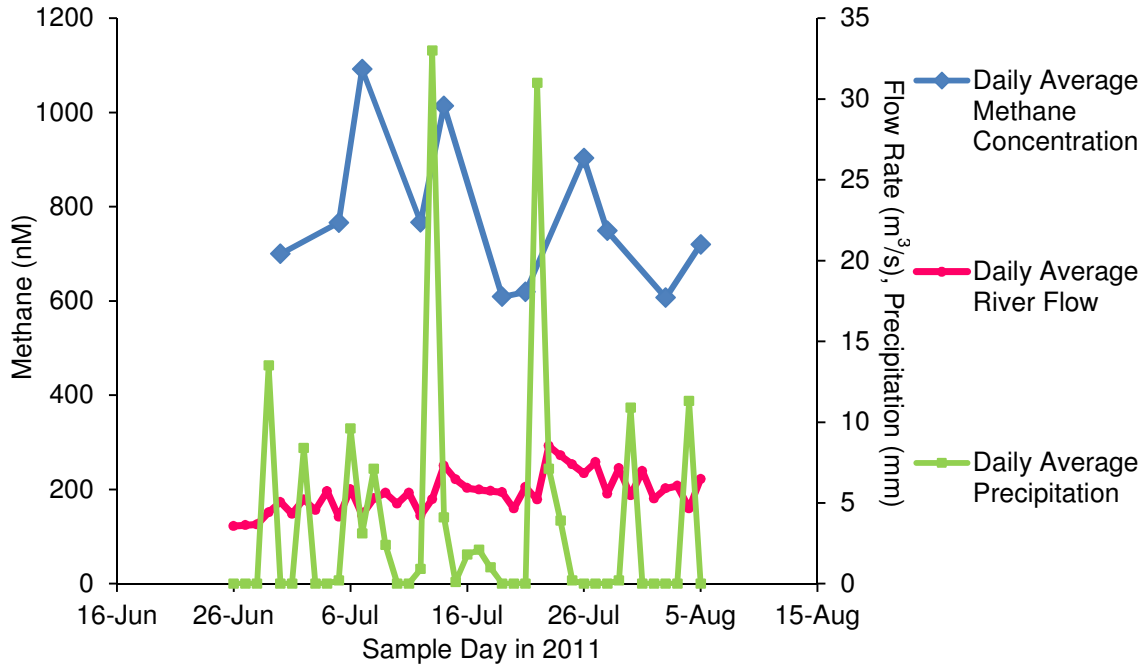

Figure 16: The largest daily average precipitation peaks tend to precede the average daily river flow rate peaks, which tend to coincide with the peaks in average daily methane concentration of the river in 2011. Note that the river flow rate and precipitation records are higher frequency than the methane record, and therefore all peaks might not match.

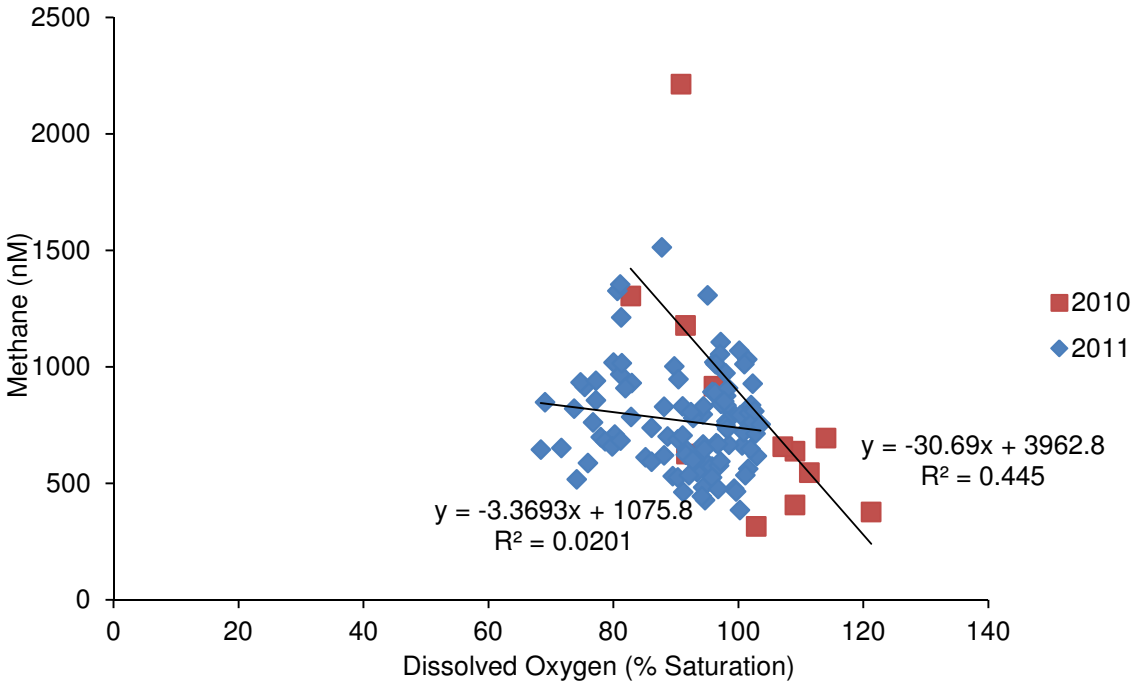

Figure 17: There appears to be a weak inverse correlation between dissolved methane and dissolved oxygen in the river water in 2010, but not in 2011.

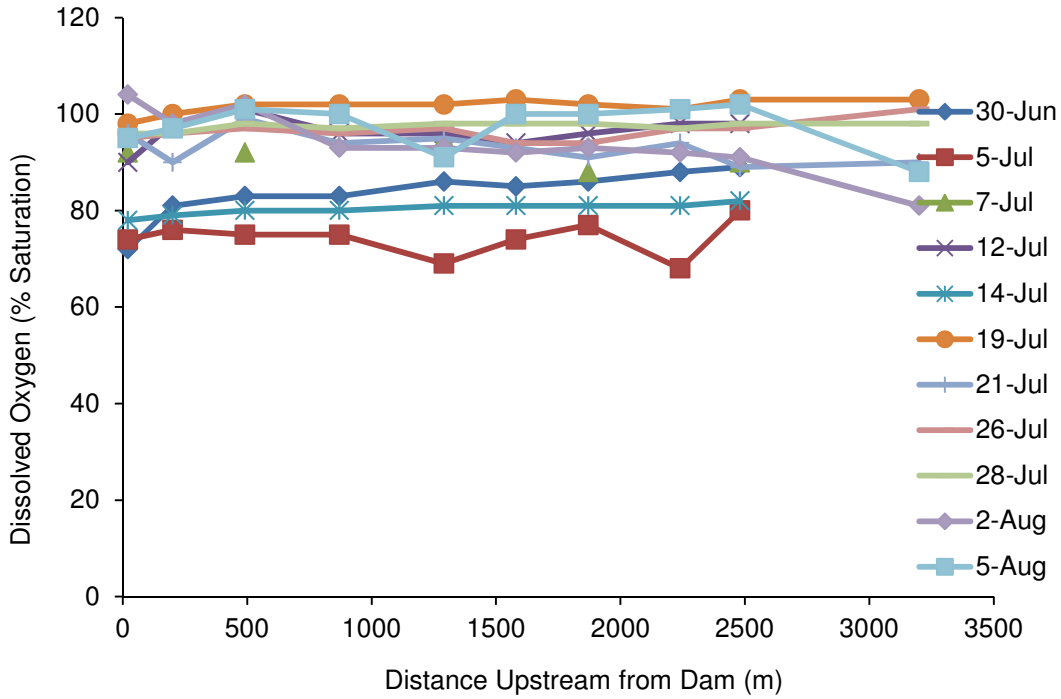

Figure 18: There does not appear to be any spatial variability of dissolved oxygen downstream toward the dam in 2011. The dam and most downstream sample site in the river (site 'Ladder 2') are represented by zero meters (the graph origin). The analytical error is ± 2%.

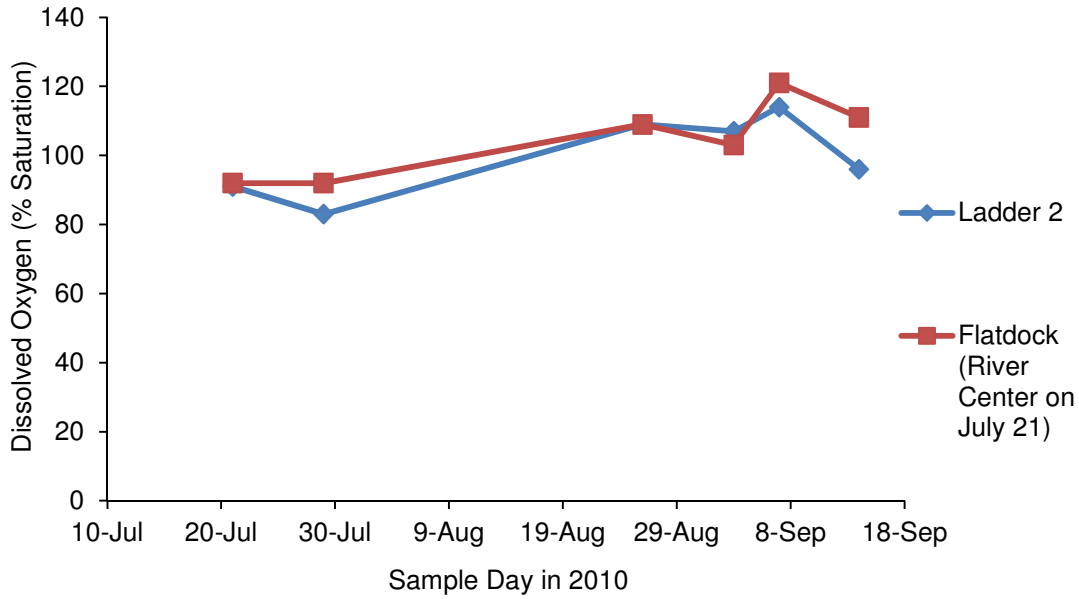

Figure 19: The dissolved oxygen concentration in the river water varies uniformly at all sample sites in the river between sampling days in 2010. The analytical error is ± 1%.

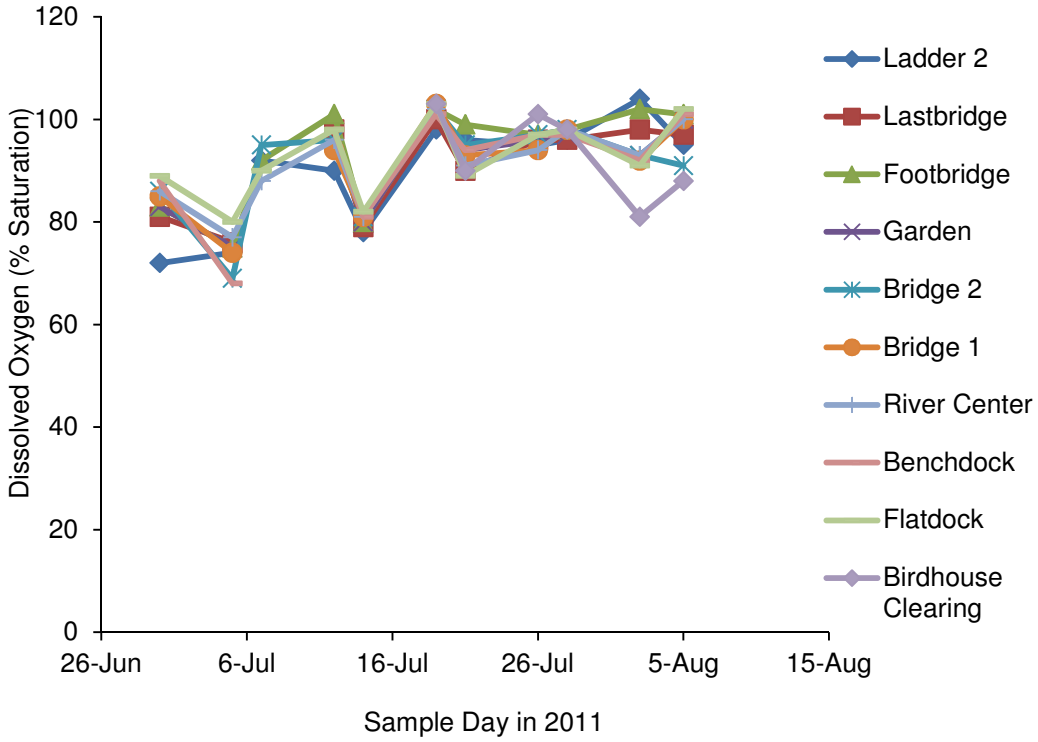

Figure 20: The dissolved oxygen concentration in the river water varies uniformly at all sample sites in the river between sampling days in 2011. The analytical error is ± 2%.

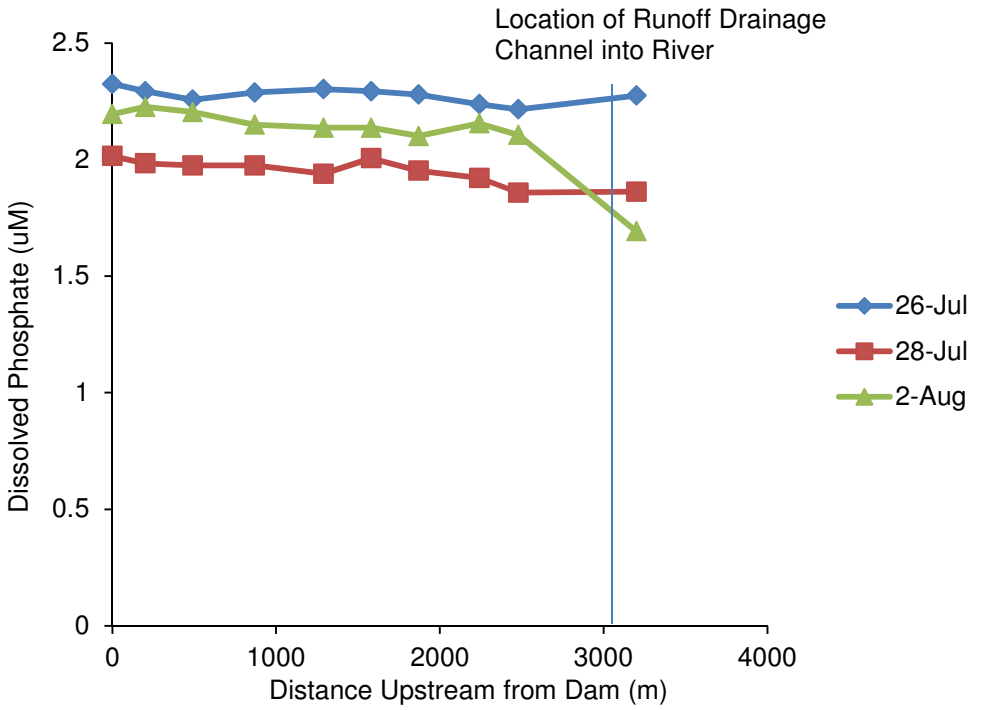

Figure 21: The dissolved phosphate concentration in the river water remains relatively constant. On August 2, 2011 there is a jump in concentration between the last two sites. The drainage channel resides between these sites, and is likely the cause of this jump in concentration.

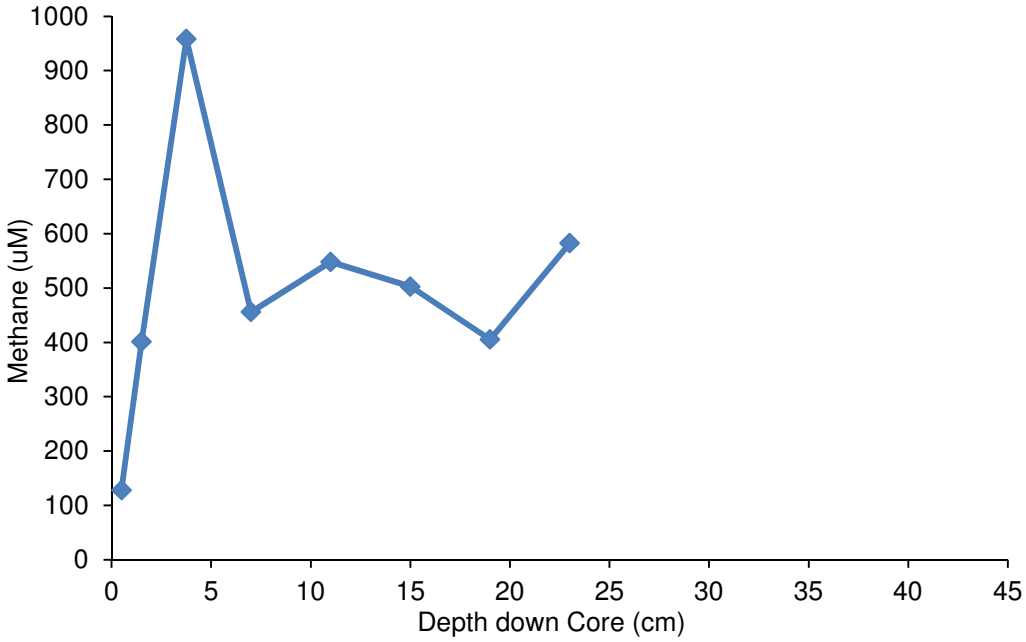

Figure 22: The dissolved methane concentration in the pore water is shown for a push core taken 15m upstream from the “Bridge 1” sample site in 2010.

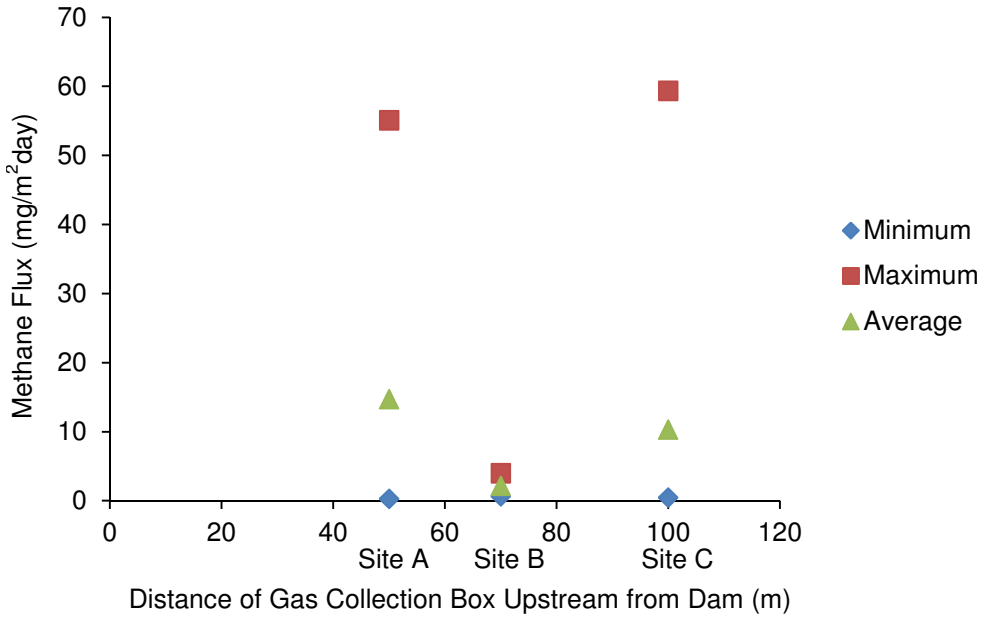

Figure 23: The range of methane flux from the river water to the atmosphere is shown at sample sites A, B, and C (see Figure 3).

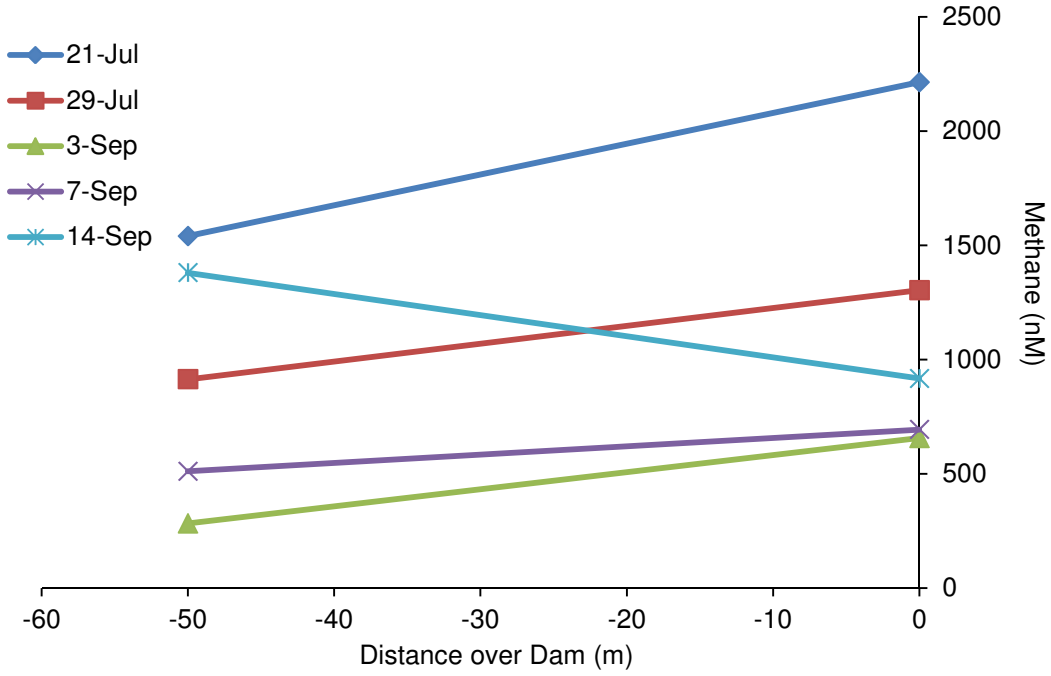

Figure 24: In 2010, the dissolved methane concentration dropped from 26-57% between the sample site immediately before the dam ('Ladder 2') and the site immediately after the dam ('Back Restaurant'), excluding the one sample day where the concentration increased 50%. The origin represents 'Ladder 2'. 'Back Restaurant' is represented by -50m on the x-axis. This figure does not take into account dilution from the fjord. The error is ± 56nM.

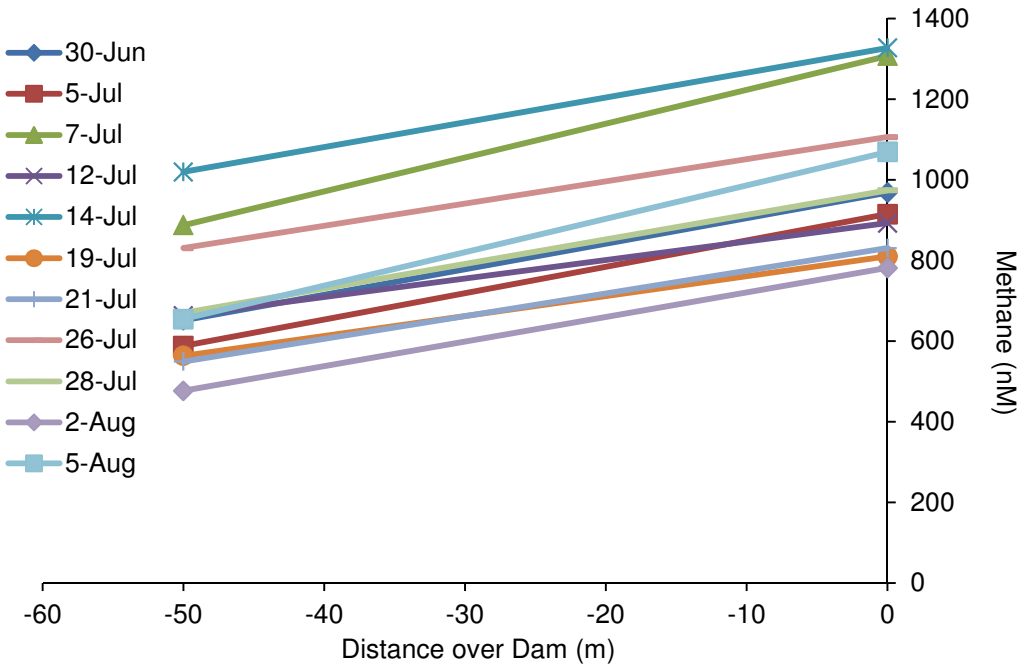

Figure 25: In 2011, the dissolved methane concentration dropped from 25-39% between the sample site immediately before the dam ('Ladder 2') and the site immediately after the dam ('Back Restaurant'). The origin represents 'Ladder 2'. 'Back Restaurant' is represented by -50m on the x-axis. This figure does not take into account dilution from the fjord. The error is ± 49nM.

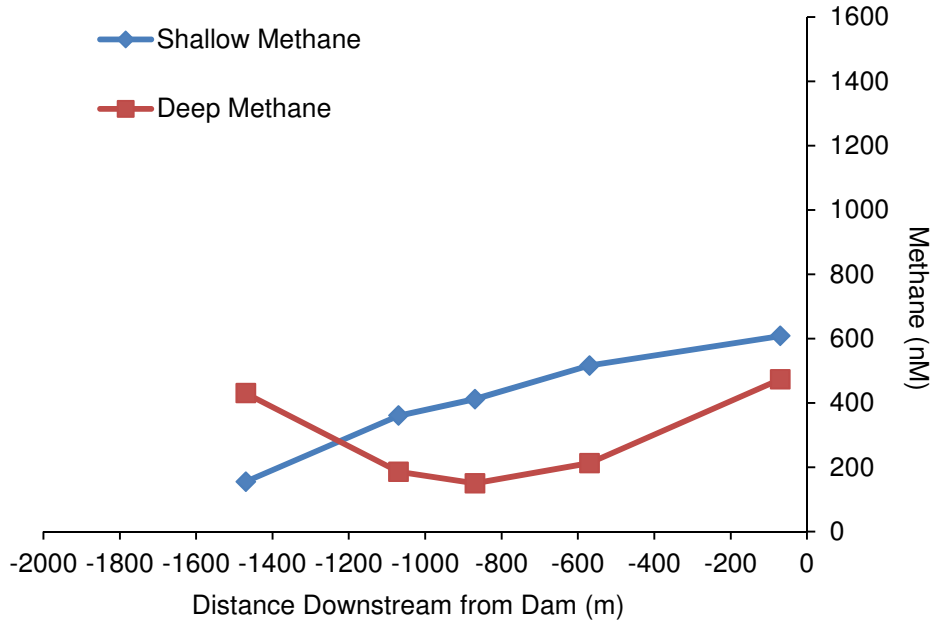

Figure 26: In the Brackish Discharge Zone in 2011, the dissolved methane concentration in the surface waters (1m bsl) decreases away from the dam (represented by the origin of the graph) out to the Kiel Fjord. The dissolved concentration in the deep waters (1.5m above the sediment-water interface) decreases away from the dam before increasing after the third sample site. See Figure 1 for water depth of each site. The standard error is ± 31nM.

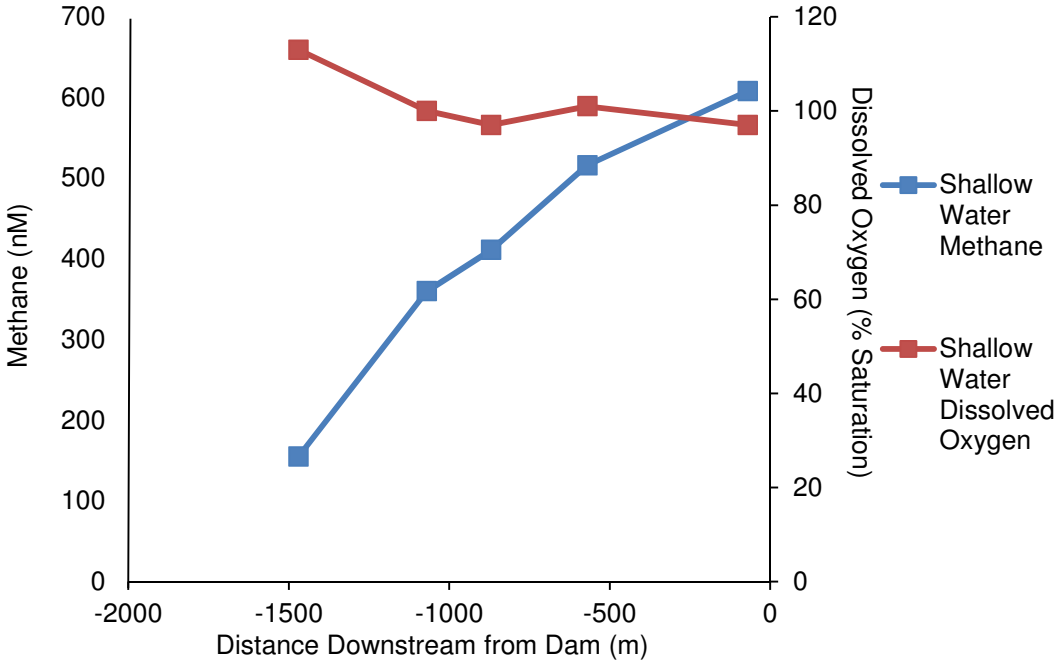

Figure 27: The dissolved methane and dissolved oxygen in the surface waters of the Brackish Discharge Zone in 2011 show opposite trends away from the dam. The standard error of methane is ± 31nM.

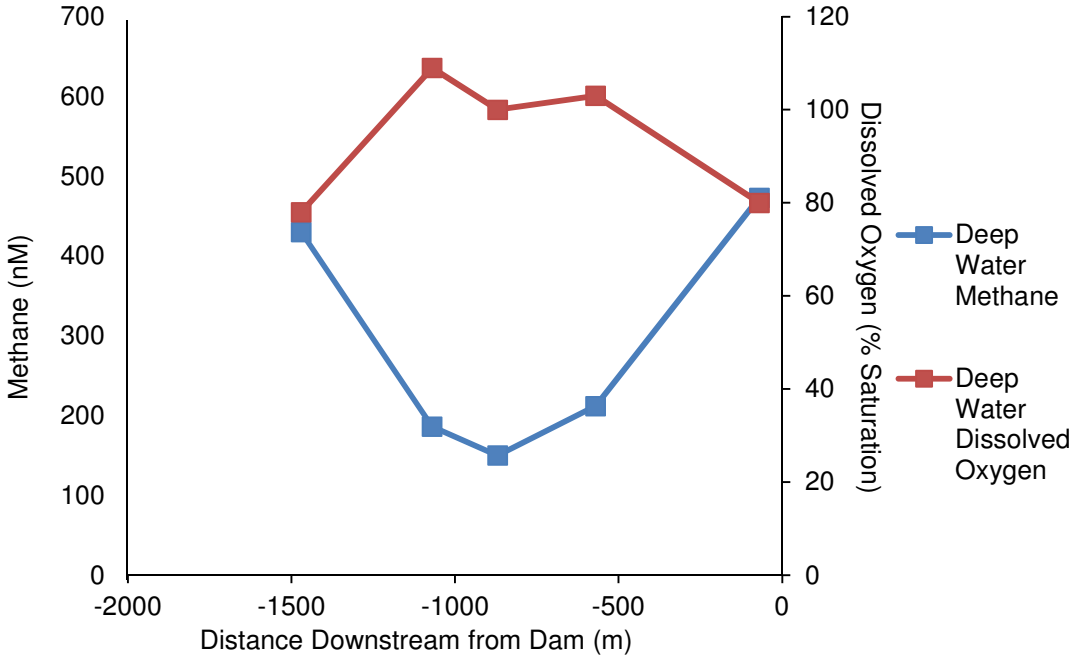

Figure 28: The deep water dissolved methane and deep water dissolved oxygen in the Brackish Discharge Zone in 2011 show opposite trends away from the dam. The standard error of methane is ± 31nM.

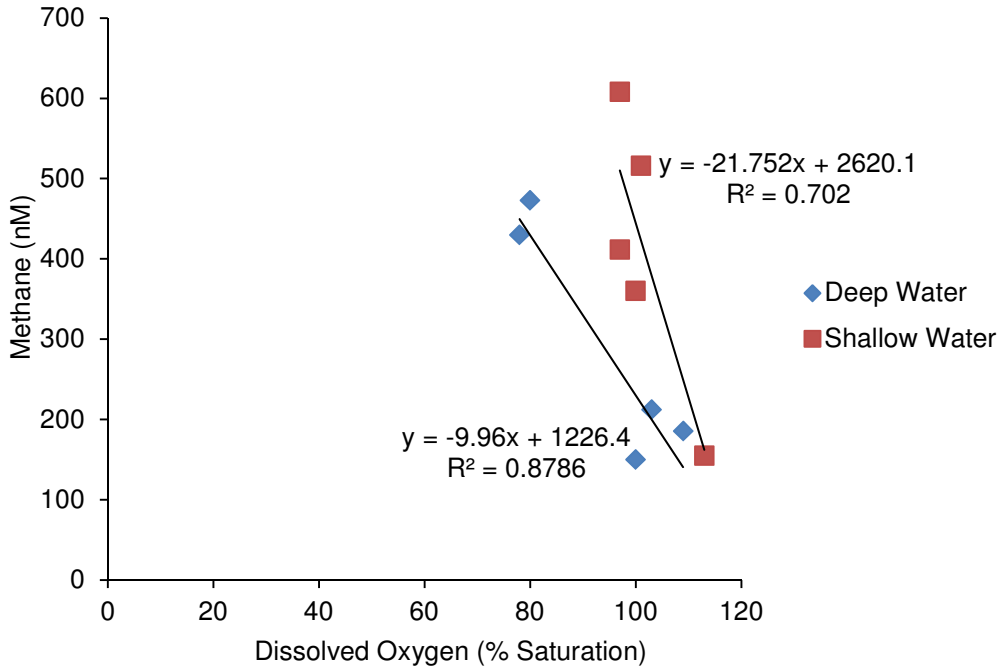

Figure 29: The dissolved methane and dissolved oxygen in the surface waters and deep waters of the Brackish Discharge Zone in 2011 correlate well. A better correlation exists in the deep waters than in the surface waters. The depths of the sample sites can be found in Figure 1.

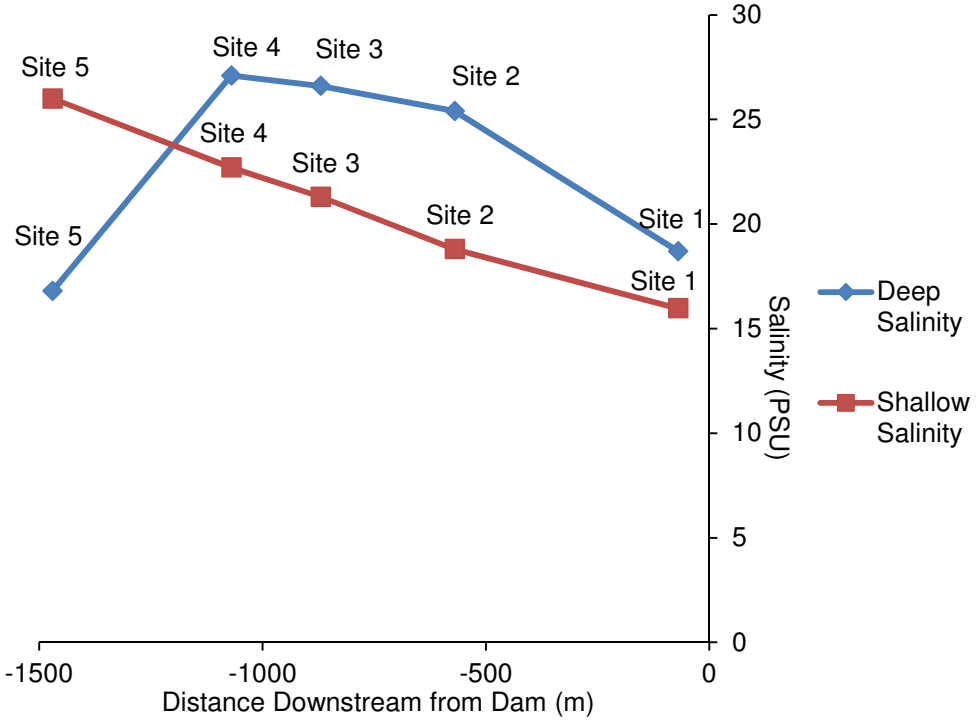

Figure 30: The salinity in the surface water (1m bsl) steadily increases away from the dam due to mixing with the fjord waters. The salinity in the deep water (1.5m above the sediment-water interface) increases, then decreases at Site 5 (see Figure 2). This may be due to a freshwater seep in the sediment.

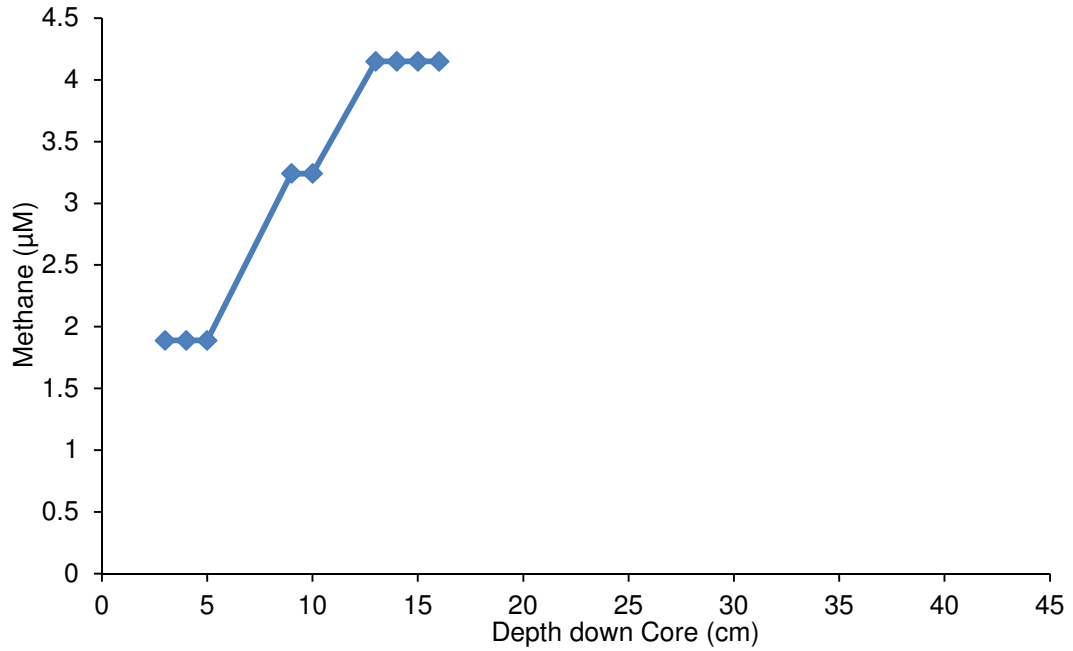

Figure 31: The dissolved methane concentration in the pore water of the Site 1 core (see Figure 2) from 2011 in the Brackish Discharge Zone is shown.

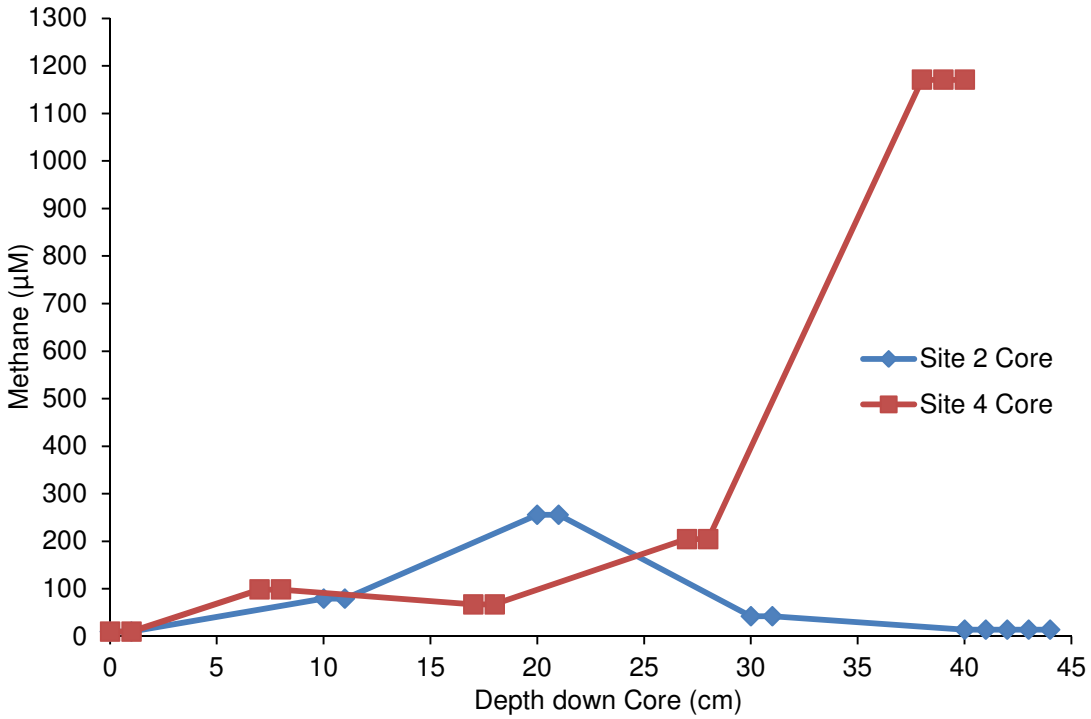

Figure 32: The dissolved methane concentration in the pore water of the Site 2 core and Site 4 core (see Figure 2) from 2011 in the Brackish Discharge Zone is shown.

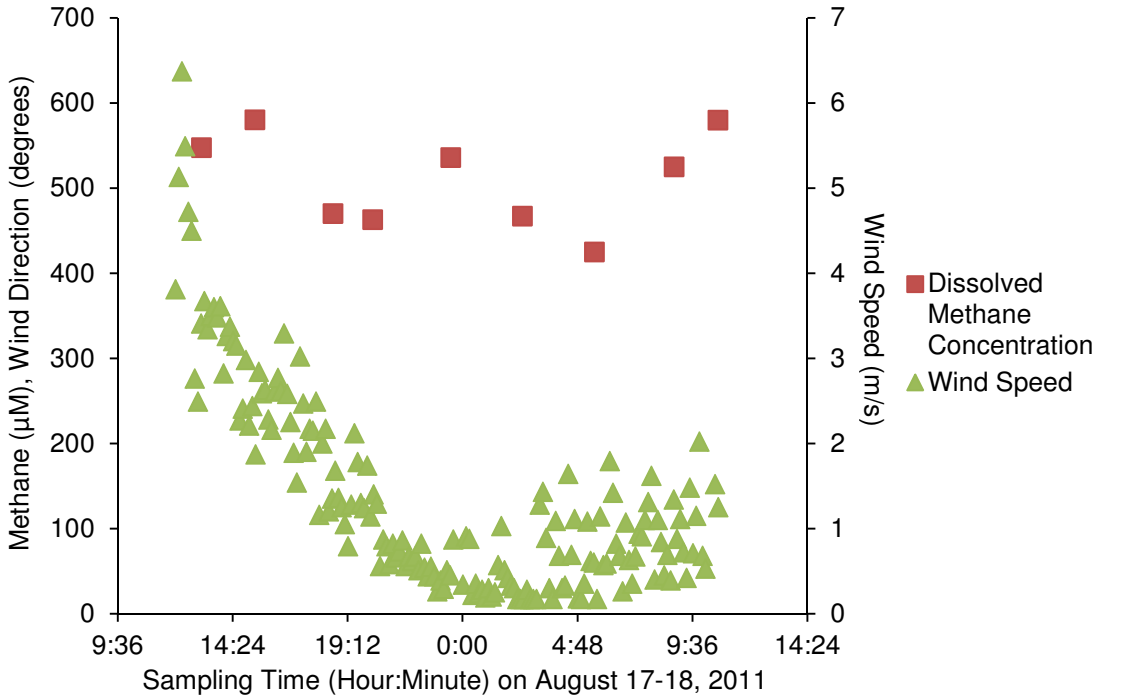

Figure 33: During the 22 hour survey on August 17-18, 2011, the winds relax around the same time that there is an evening peak in methane concentration in the surface water at 'Ladder 2'. The methane error is ± 43nM.

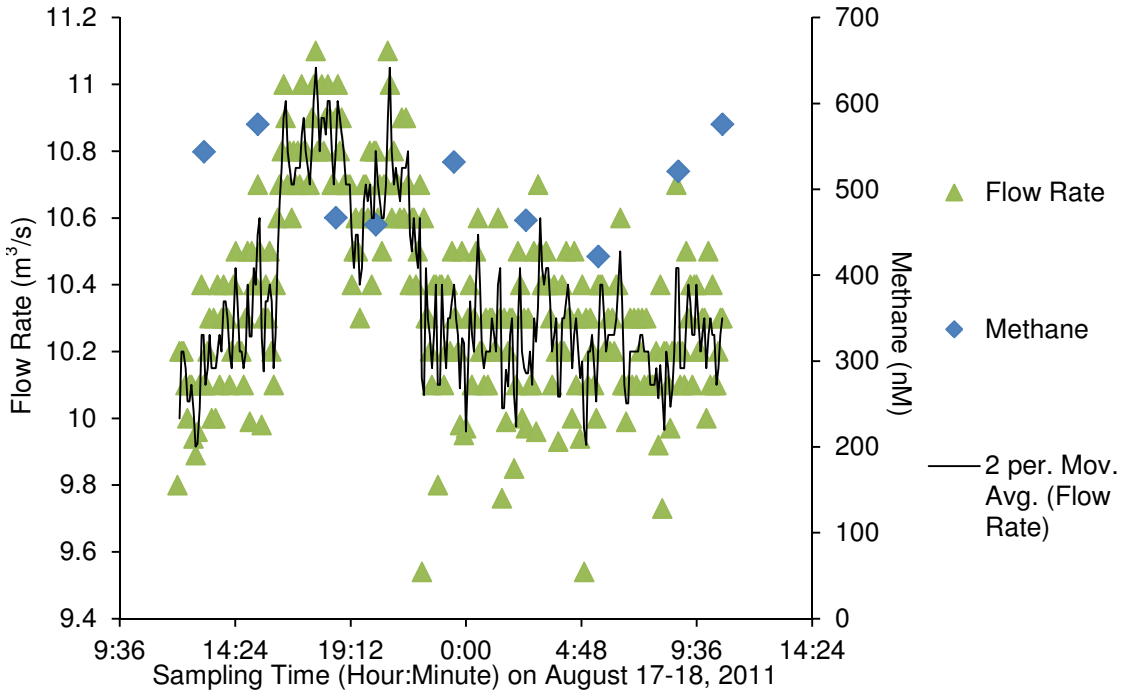

Figure 34: During the 22 hour survey on August 17-18, 2011, there is a significant peak in flow rate before the evening drop in methane concentration in the surface water at 'Ladder 2' at 18:36 and 20:15. This increase in flow rate may be due to an opening of the dam, which may result in lower methane concentration water upstream being brought downstream to 'Ladder 2'. The error in methane is ± 43nM.

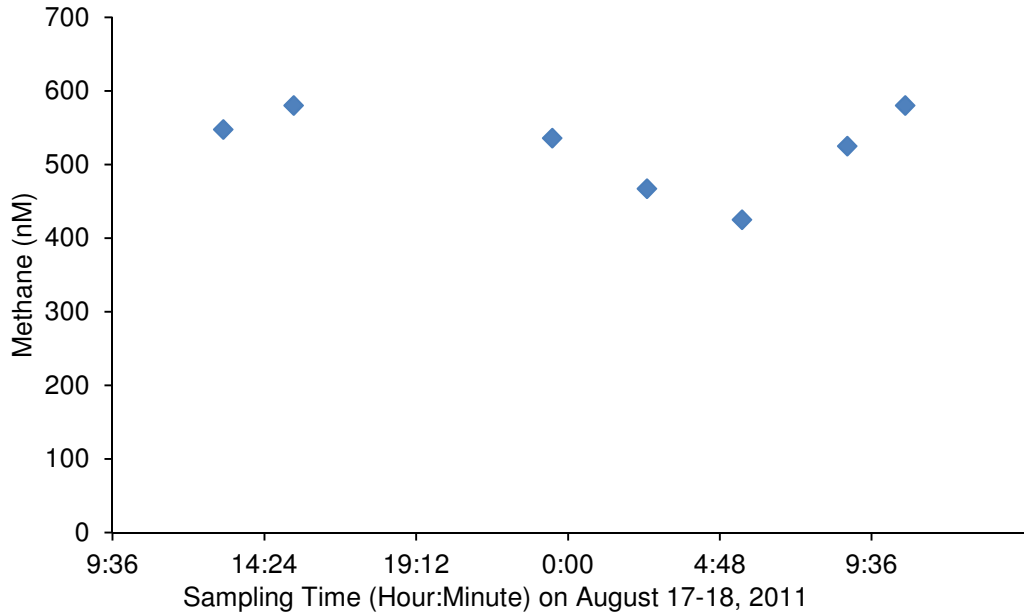

Figure 35: If the methane measurements at 'Ladder 2' forming the evening trough at 18:36 and 20:15 are removed, a smooth diurnal cycle is seen in the 22 hour survey data on August 17-18, 2011. The error in methane is ± 43nM.

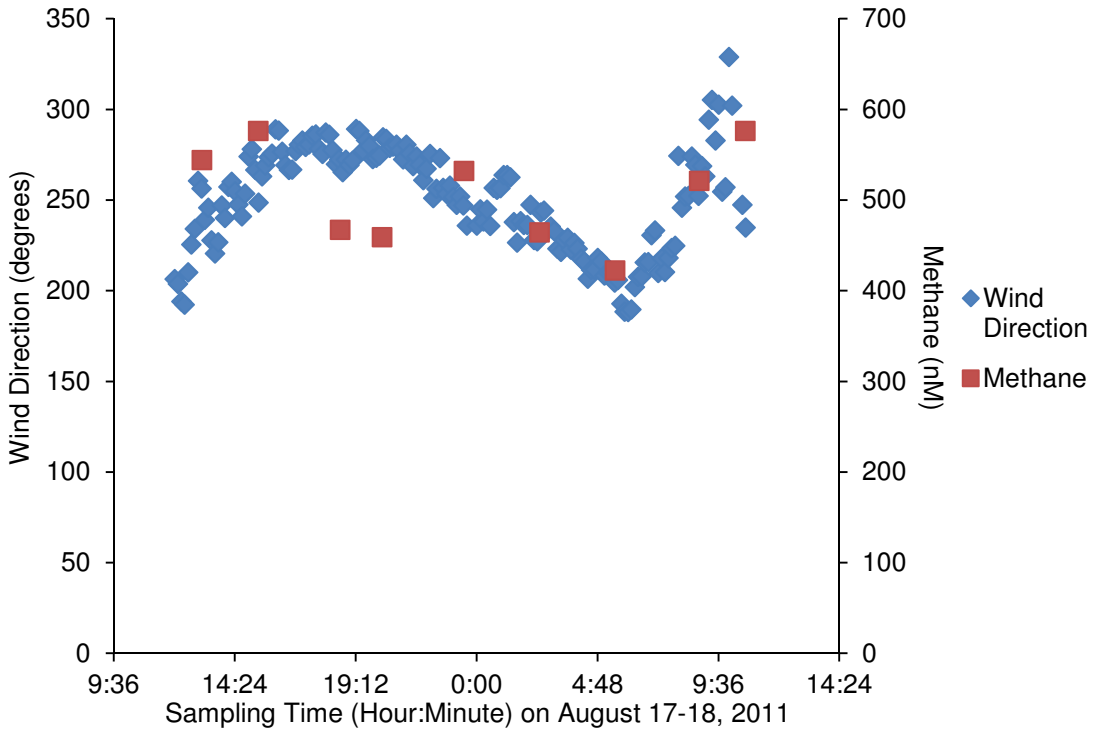

Figure 36: During the 22 hour survey on August 17-18, 2011, there is an evening shift in wind direction from onshore to offshore. The change in wind direction appears to occur a similar time there is change in the methane concentration trend in the surface waters at 'Ladder 2'. The error in methane is ± 43nM.

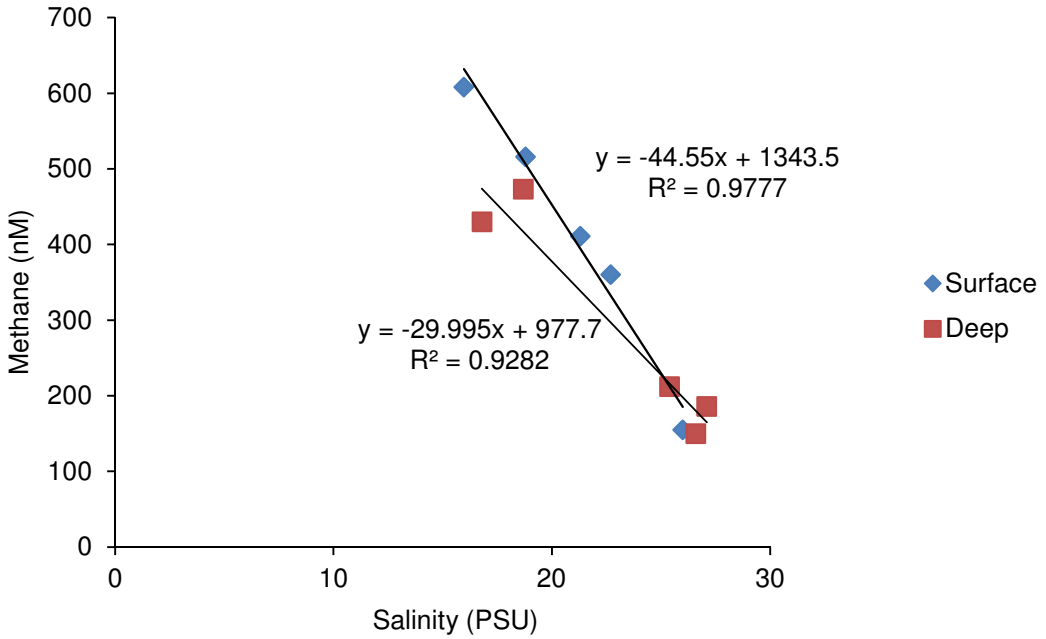

Figure 37: Methane correlates well with salinity in the Brackish Discharge Zone surface and deep waters.

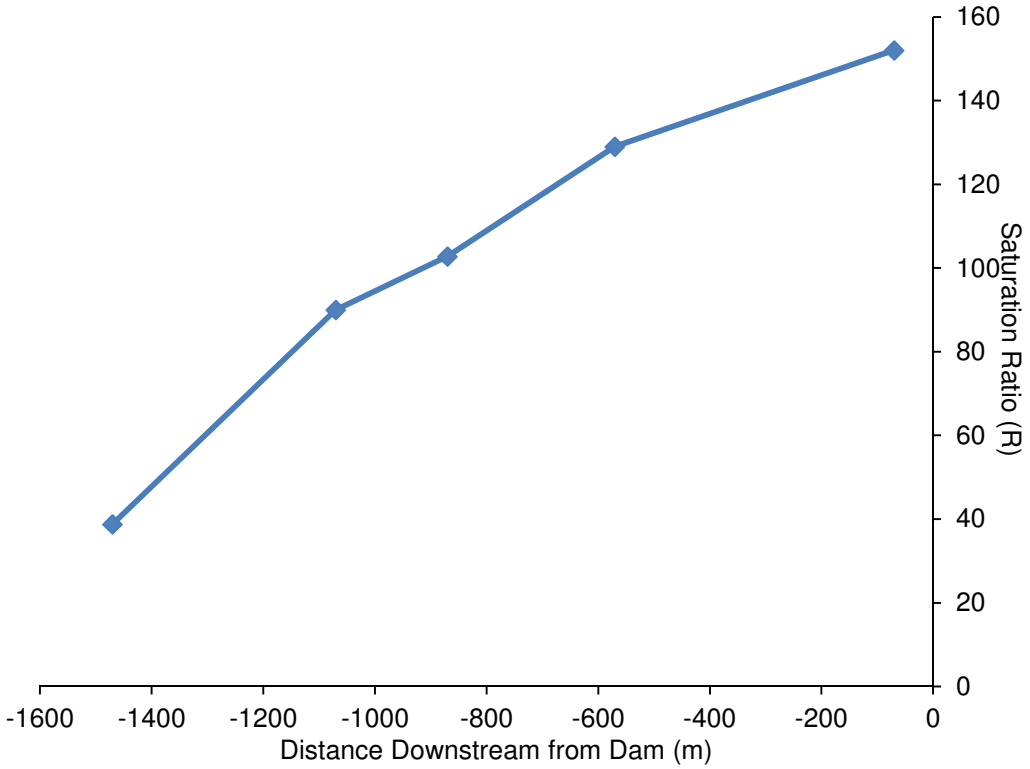

Figure 38: The saturation ratio (R), calculated by the methane concentration, salinity, and temperature data collected during the 22 hour survey on August 17-18, 2011, decreases away from the dam in the Brackish Discharge Zone.

Table 1: Distance of Sample Sites from Dam

Sample Site	Distance from Dam (m) (negative=downstream) (positive=upstream)
Birdhouse Clearing	3200
Drainage	3100
Flatdock	2480
Benchdock	2240
River Center	1870
Bridge 1	1580
Bridge 2	1290
Garden	870
Footbridge	490
Last Bridge	200
Ladder 2	0
Back Restaurant	-50
Site 1	-70
Site 2	-570
Site 3	-870
Site 4	-1070
Site 5	-1470

Table 2: River Methane Concentration Summary (modified from Scranton and McShane, 1991).

River	Methane Concentration (nM)	Reference
Potomac River	1700	Lamontagne et al. (1973)
Chesapeake Bay	17-58	Lamontagne et al. (1973)
York River	37-39	Lamontagne et al. (1973)
Mississippi River	107-366	Swinnerton and Lamontagne (1974)
Sepik River (New Guinea)	87-133	Wilkniss et al. 1978)
Yaquina River (head of estuary) (stations along river)	 300-1000 276-1730	 Butler et al. (1987) De Angelis and Lilley (1987)
Alsea River	22-729	De Angelis and Lilley (1987)
Siletz River	500-1100	De Angelis and Lilley (1987)
McKenzie River (Cascade Range) (Willamette Valley)	 5-79 1018	 De Angelis and Lilley (1987)
Willamette River	155-298	De Angelis and Lilley (1987)
Amazon River (main stem) (varzea)	 50 12,000	 Richey et al. (1988)
Rhine (predicted from Scranton and McShane, 1991)	50-150	Scranton and McShane (1991)
Western Scheldt (predicted from Scranton and McShane, 1991)	500-5000	Scranton and McShane (1991)
Schwentine	316-2213 ± 51	This Study

Table 3: The methane concentrations (nM) of two samples (one duplicate) are shown for each sample site on each sample day in 2010. The standard error for these samples is 30nM. The analytical error for these samples is approximately 20nM.

Dissolved Methane (nM) in River and Outlet in 2010 Error = ± 51 nM (river samples), Error = ± 51 nM ('Back Restaurant' site)							
	21-Jul	**29-Jul**	**26-Aug**	**3-Sep**	**7-Sep**	**14-Sep**	**Average Site Concentration**
Back Restaurant**	1522 1559	967 860	n/a	466 392	505 517	1382 1378	925
Ladder 2	2170 2257	1247 1361	663 613	659 655	677 711	933 902	1071
Last Bridge	1940*	1773*	597 535	626 644	664 690	959 960	1092
Footbridge	1717*	1176*	637 580	563 543	738 680	958 935	952
Garden	1795*	1165*	412 530	544 570	582 609	1045 1042	938
Bridge 2	1298*	1063*	491 499	460 455	542 536	709 705	760
Bridge 1	n/a	827*	445 420	415 384	477 459	689 643	558
River Center	1178	710*	397 406	367 362	444 428	583 603	614
Bench Dock	n/a	640*	382 379	313 331	372 414	588 606	466
Flatdock	n/a	626*	419 396	321 311	366 391	541 551	455

*These samples did not have a duplicate; therefore one sample concentration is reported.
** This sample site is not included in the River Average Daily Concentration.

Table 4: The dissolved oxygen concentrations of two samples (one duplicate) are shown for two sample sites on each sample day in 2010. The analytical error for these samples is approximately 2%.

Dissolved Oxygen (% Saturation) in River in 2010 An. Error = ± 1%						
	21-Jul	**29-Jul**	**26-Aug**	**3-Sep**	**7-Sep**	**14-Sep**
Ladder 2	91*	83*	109*	107 107	114 114	96 96
Flatdock	92*,**	92*	109*	102 104	121*	112 111

*These samples did not have a duplicate; therefore one sample concentration is reported.
**This sample was not taken at Flatdock, it was taken at River Center.

Table 5: The average temperature in the river is shown for each sample day. The temperature at each river site sampled for methane that day is included in the average.

Average Daily Temperature (Celsius) in River in 2010					
21-Jul	**29-Jul**	**26-Aug**	**3-Sep**	**7-Sep**	**14-Sep**
29.5	24.6	24.5	23.9	22.8	23.3

Table 6: The methane concentration in the pore water of the core taken 15m upstream from the 'Bridge 1' sample site on September 17, 2010 is shown.

Methane Concentration in Pore Water of River Core in 2010	
Depth down Core (cm)	**Methane in Pore Water (µM)**
1	111
1	146
2	368
3	435
4	941
5	880
7	433
9	475
11	653
13	388
15	478
17	477
19	405
23	582
25	525

Table 7: The velocity measured for each orange test used to calculate the river flow rate in 2010 is shown.

River Flow Rate Tests 2010			
Trial	**Velocity (m/s)**	**Distance**	**River Averaged Cross Sectional Area (m^2)**
1	0.06	29.5	43.23
2	0.09	29.5	43.23
3	0.08	29.5	43.23

Table 8: The methane concentrations (nM) of two samples (one duplicate) are shown for each sample site on each sample day in 2011. The sites in the Brackish Discharge Zone (Site 1-5), are reported in Data Set 12. The standard error for these samples is 30nM. The analytical error for these samples is approximately 17nM.

Dissolved Methane (nM) in River and Outlet in 2011 Error = ±47 (river samples), Error = ±51nM ('Back Restaurant' site), Error = ±328 ('Drainage' site)							
	30-Jun	**5-Jul**	**7-Jul**	**12-Jul**	**14-Jul**	**19-Jul**	**21-Jul**
Back Restaurant**	660 643	579 597	890 884	628 698	989 1049	553 574	536 562

Table 8 (continued)

Ladder 2	978 959	914 915	1313 1301	865 920	1451 1360	802 818	830 831
Last Bridge	932 930	915 953	1287 1296	994 1046	1313 1396	791 714	835 757
Footbridge	835 735	843 853	1507 1518	406 929	1153 1270	737 702	712 690
Garden	737 741	817 824	1095 1122	931 415	1174 859	734 693	681 697
Bridge 2	614 611	756 767	1006 999	836 833	1043 775	636 600	576 589
Bridge 1	611 575	651 638	981 984	767 769	885 867	545 586	587 558
River Center	673 568	709 711	976 920	709 688	864 723	516 533	573 580
Bench Dock	521 540	649 634	867 841	695 668	857 814	485 471	528 523
Flatdock	518 517	624 622	857 792	659*	801 806	494 472	488 464
Drainage**	n/a	n/a	n/a	n/a	n/a	n/a	n/a
Birdhouse Clearing	n/a	n/a	n/a	n/a	n/a	447 410	445 443

Dissolved Methane (nM) in River and Outlet in 2011 (continued)				
	26-Jul	**28-Jul**	**2-Aug**	**5-Aug**
Back Restaurant**	867 794	637 701	463 491	679 630
Ladder 2	1114 1098	1015 932	760 802	1075 1063
Last Bridge	1060 1050	952 927	794 818	1020 1004
Footbridge	1003 1061	852 845	642 768	913 944
Garden	1025 998	858 855	642 726	824 833
Bridge 2	879 900	749 759	650 642	706 666
Bridge 1	908 910	740 726	589 599	625 635
River Center	833 850	658 639	542 529	583 602
Bench Dock	780 751	596 598	459 471	538 624
Flatdock	742 758	595 605	455 470	517 516
Drainage**	n/a	909 1884	4894 5297	19264 18861
Birdhouse Clearing	708 624	532 538	387 386	418 390

** These sample sites are not included in the River Average Daily Concentration.

Table 9: The dissolved oxygen concentrations of two samples (one duplicate) are shown for each sample site on each sample day in 2011.

Dissolved Oxygen (% Saturation) in River in 2011 An. Error = ±2%							
	30-Jun	**5-Jul**	**7-Jul**	**12-Jul**	**14-Jul**	**19-Jul**	**21-Jul**
Back Restaurant**	71*	76 72	n/a	97 96	84 85	85 87	85 92
Ladder 2	72*	74 74	92 91	90 91	78 78	98 98	96 96
Last Bridge	81*	76 76	n/a	101 95	79 79	101 100	90 91
Footbridge	83*	79 72	87 96	103 98	80 80	103 101	98 101
Garden	83*	71 78	n/a	94 98	80 80	102 101	87 102
Bridge 2	86*	59 79	94 96	96 97	81 81	101 102	99 90
Bridge 1	85*	75 73	n/a	93 96	81 81	102 103	92 95
River Center	86*	76 78	86 89	96 97	81 82	100 103	84 98
Bench Dock	88*	69 68	n/a	99 97	81 81	101 100	94 95
Flatdock	89*	78 82	96 84	98 99	82 82	103*	86 91
Drainage**	n/a	n/a	n/a	n/a	n/a	n/a	n/a
Birdhouse Clearing	n/a	n/a	n/a	n/a	n/a	103*	91 90

Dissolved Oxygen (% Saturation) in River in 2011 (continued)				
	26-Jul	**28-Jul**	**2-Aug**	**5-Aug**
Back Restaurant**	99 101	100 105	103 101	73*
Ladder 2	96 94	95 97	105 102	94 95
Last Bridge	96 95	96 96	100 96	99 95
Footbridge	97 97	98 99	102 101	101 101
Garden	96*	97 97	93 93	100 99
Bridge 2	97 96	98 98	93 93	99 84
Bridge 1	92 96	100 96	92 92	101 100
River Center	96 93	98 99	91 94	100 100
Bench Dock	97 97	96 98	92 93	101 101
Flatdock	97 97	96 100	91 91	102 103

Table 9 (continued)

Drainage**	n/a	77 78	83 83	70*
Birdhouse Clearing	101*	99 97	81 81	86 90

* These samples did not have a duplicate; therefore one sample concentration is reported.
** These sample sites are not included in the River Average Daily Concentration

Table 10: The average temperature in the river is shown for each sample day. The temperature at each river site sampled for methane that day is included in the average.

Average Daily Temperature (Celsius) in River in 2011										
30-Jun	**5-Jul**	**7-Jul**	**12-Jul**	**14-Jul**	**19-Jul**	**21-Jul**	**26-Jul**	**28-Jul**	**2-Aug**	**5-Aug**
20.6	17.3	19.6	20.9	19.2	19.2	19.9	16.7	18.7	19.9	20.6

Table 11: The dissolved phosphate (filtered water samples) concentrations in the river are shown.

Dissolved Phosphate in River in 2011 (µM)			
	26-Jul	**28-Jul**	**2-Aug**
Birdhouse Clearing	2.275	1.862	1.693
Flatdock	2.216	1.858	2.106
Benchdock	2.238	1.921	2.155
River Center	2.279	1.952	2.101
Bridge 1	2.293	2.006	2.137
Bridge 2	2.302	1.939	2.137
Garden	2.288	1.975	2.15
Footbridge	2.257	1.975	2.204
Lastbridge	2.293	1.984	2.226
Ladder 2	2.325	2.015	2.195

Table 12: The methane concentrations (nM) of two samples (one duplicate) are shown for each measurement during the 22 hour survey in 2011.

Dissolved Methane (nM) over 22 Hour Survey in 2011 Error = ± 43	
Time	**Methane Concentration (nM)**
13:06	544 543
15:20	599 552
18:35	476 458
20:15	483 436

Table 12 (continued)

23:30	532 531
2:30	458 470
5:30	407 438
8:50	513 530
10:40	552 599

Table 13: A list of the rate of concentration change measurements in the gas collection boxes deployed on August 17-18, 2011 is shown.

Measurements of Flux of Methane from River to Atmosphere			
Distance of Gas Collection Box Upstream from Dam (m)	**50**	**70**	**100**
Rate of Methane Concentration Change in Box (mg/m^2day)	0.29	1.84	0.77
	4.15	3.98	2.27
	5.91	0.65	4.04
	2.87	1.96	0.45
	15.78		5.44
	10.5		8.23
	55.11		3.33
	0.32		8.05
	37.1		11.06
			59.34
Average	14.67	2.1075	10.298
Standard Deviation	19.02786	1.381289	17.57068

Table 14: Water column data collected during the Brackish Discharge Zone Cruise on July 17, 2011 are shown. One sample was taken at each site and depth. The standard error for the methane concentration is 30nM.

Water Column Data from the Brackish Discharge Zone Cruise on July 17, 2011						
Site	**Depth (mbsl)**	**Distance from Dam (m)**	**Salinity (PSU)**	**Temperature**	**Methane (nM) An. Error = ± 31nM**	**Dissolved Oxygen (% Saturation)**
1	1	-70	15.97	18.3	608	97%
1	2.5	-70	18.7	17.8	473	80%
2	1	-570	18.8	18.3	516	101%

Table 14 (continued)

2	4.5	-570	25.4	17.9	212	103%
3	1	-870	21.3	18.1	411	97%
3	6.5	-870	26.6	17.8	150	100%
4	1	-1070	22.7	18.4	360	100%
4	8	-1070	27.1	17.7	186	109%
5	1	-1470	26	20.5	155	113%
5	12.5	-1470	16.8	16.8	430	78%

Table 15: The methane concentration in the cores from the Brackish Discharge Zone Cruise on July 17, 2011 is shown. One sample was taken at each depth in the core. Duplicate samples were not taken so no analytical error is available.

Methane Concentration in Pore Water of Cores from Brackish Discharge Zone Cruise on July 17, 2011		
	Depth in Core (cm)	CH4 (µM)
Site 1	3-6	2.131
	9-10	2.637
	13-16	3.739
Site 2	0-1	9.276
	10-11	65.058
	20-21	202.774
	30-31	47.510
	40-44	13.936
Site 4	0-1	9.952
	7-8	92.968
	17-18	69.240
	27-28	190.342
	38-40	862.463

REFERENCES

Abril, G., Guérin, F., Richard, S., Delmas, R., Galy-Lacaux, C., Gosse, P., Tremblay, A., Varfalvy, L., Dos Santos, M. A., and Matvienko, B., 2005. Carbon dioxide and methane emissions and the carbon budget of a 10-year old tropical reservoir (Petit Saut, French Guiana). Global Biogeochemical Cycles, v. 19, GB4007.

Armstrong, J., and Armstrong, W., 1990. Light-enhanced convective throughflow increase oxygenation in rhizomes and rhizosphere of *Phragmites australis* (Cav.) Trin. Ex Steud. New Phytologist, v. 114, no. 1, pp. 121-128.

Bange, H., Bartell, U. H., Rapsomanikis, S., and Andreae, M. O., 1994. Methane in the Baltic and North Seas and a reassessment of the marine emissions of methane. Global Biogeochemical Cycles, v. 8, pp. 465-480.

Bastviken, D., Cole, J. J., Pace, M.L., and Tranvik, L. J., 2004. Methane emissions from lakes: Dependence of lake characteristics, two regional assessments, and a global estimate. Global Biogeochemical Cycles, v. 18, GB4009.

Bastviken, D., Tranvik, L. J., Downing, J. A., Crill, P. M., and Enrich-Prast, A., 2011. Freshwater Methane Emissions Offset the Continental Carbon Sink. Science, v. 331, p. 50.

Bernet Catch Regional Report: Schwentine River, Water Management Plan, Provisional Management Plan Pursuant to the EU Water Framework Directive, 2006: http://bernet.naturstyrelsen.dk/NR/rdonlyres/6F8B247F-A2B1-4E17-BCD2-0F8B9F5A48CB/0/SH_PRB_managemant_plan.pdf.

Brix, H., Sorrell, B. K., and Orr, P. T., 1992. Internal pressurization and convective gas flow in some emergent freshwater macrophytes. Limnology and Oceanography, v. 37, pp. 1420-1433.

Brunke, M., 2004. Stream typology and lake outlets – a perspective towards validation and assessment from northern Germany (Schleswig-Holstein). Limnologica – Ecology and Management of Inland Waters, v. 34, issue 4, pp. 460-478.

Chanton, J. P., Whiting, G. J., Happell, J. D., and Gerard, G., 1993. Contrasting rates and diurnal patterns of methane emissions from emergent aquatic macrophytes. Aquatic Botany, v. 46, pp. 111–128.

Chanton, J. P., and Whiting, G. J., 1996. Methane stable isotopic distributions as indicators of gas transport mechanisms in emergent aquatic plants. Aquatic Botany, v. 54, pp. 227-236.

Cicerone, R. J., and Oremland, R. S., 1988. Biogeochemical aspects of atmospheric methane. Global Biogeochemical Cycles, v. 2, pp. 299-327.

Cicerone, R. J., and Shetter, J., 1981. Sources of atmospheric methane: Measurements in rice paddies and a discussion. Journal of Geophysical Research, v. 86, issue C8, p. 7203.

Dacey, J. W. H., 1981a. Pressurized ventilation in the yellow waterlily. Ecology, v. 62, pp. 1137-1147.

Dacey, J. W. H., 1981b. How aquatic plants ventilate. Oceanus, v. 24, pp. 43-51.

Dacey, J. W. H., and Klug, M. J., 1982. Floating leaves and nighttime ventilation in *Nuphar*. American Journal of Botany, v. 69, pp. 999-1003.

de Angelis, M. A., and Lilley, M. D., 1987. Methane in surface waters of Oregon Estuaries and Rivers. Limnology and Oceanography, v. 32, no. 3, pp. 716-722.

de Angelis, M. A., and Scranton, M. I., 1993. Fate of methane in the Hudson river and estuary. Global Biogeochemical Cycles, v. 7, pp. 509-523.

Delsontro, T., McGinnis, D. F., Sobek, S., Ostrovsky, I., and Wehrli, B., 2010. Extreme methane emissions from a Swiss hydropower reservoir: contribution from bubbling sediments. Environmental Science & Technology, v. 44, pp. 2419-2425.

Deutscher Wetterdienst, 2011. Climate Data Online Database: http://www.dwd.de (accessed February 2012).

Duan, Z. and Mao, S., 2006. A thermodynamic model for calculating methane solubility, density, and gas phase composition of methane-bearing aqueous fluids from 273 to 523 K and from 1 to 1000 bar. Geochimica et Cosmochimica, v. 70, pp. 3369-3386.

Fearnside, P. M., 2002. Greenhouse gas emissions from a hydroelectric reservoir (Brazil's Tucuruí Dam) and the energy policy implications. Water Air Soil Pollution, v. 133, pp. 69-96.

Fearnside, P. M., 2004. Greenhouse gas emissions from hydroelectric dams: controversies provide a springboard for rethinking a supposedly clean energy source. Climate Change, v. 66, pp. 1-8.

Fearnside, P. M., 2005a. Do hydroelectric dams mitigate global warming? The case of Brazil's Curuá-Una Dam. Mitigation and Adaptation Strategies for Global Change, v. 10, pp. 675-691.

Fearnside, P. M., 2005b. Brazil's Samuel Dam: lessons for hydroelectric development policy and the environment in Amazonia. Environmental Management, v. 35, pp. 1-19.

Galy-Lacaux, C., Delmas, R., Jambert, C., Dumestre, J. F., Labroue, L., Richard, S., and Gosse, P., 1997. Gaseous emissions and oxygen consumption in hydroelectric dams: A case study in French Guiana. Global Biogeochemical Cycles, v. 11, pp. 471-483.

Galy-Lacaux, C., Delmas, R., Kouadio, G., Richard, S., and Gosse, P., 1999. Long-term greenhouse gas emissions from hydroelectric reservoirs in tropical forest regions. Global Biogeochemical Cycles, v. 13, pp. 503-517.

Grosse, W., and Mevi-Shutz, J., 1987. A beneficial gas transport system in *Nymphoides peltata*. American Journal of Botany, v. 74, pp. 947-952.

Harriss, R. C. and Sebacher, D. I., 1981. Methane flux in forested freshwater swamps of the southeastern United States. Geophysical Research Letters, v. 8, pp. 1002-1004.

Houghton, J. T., Jenkins, G. J., and Ephraums, J. J. (Eds.), 1990. Climate Change: The IPCC Scientific Assessment: Cambridge University Press, New York, pp. 365.

Pachauri, R.K., and Reisinger, A. (Eds.), 2007. IPCC Synthesis Report, Geneva, Switzerland, pp. 104.

IFM-Geomar Leibniz Institute of Marine Sciences, 2011, Overview Geobiochemical Analysis Online Resource: http://www.ifm-geomar.de/index.php?id=mg_sauerstoff&L=1 (accessed July 2011).

IFM-Geomar Leibniz Institute of Marine Sciences, 2011, Overview Geobiochemical Analysis Online Resource: http://www.ifm-geomar.de/index.php?id=mg_chlorid (accessed July 2011).

Marine Meteorology, Helmholtz Centre for Ocean Research Kiel (IFM-Geomar) Weather Records, 2011. Pers. Comm. Frauke Nevoigt.

Climate Change 2007: Synthesis Report, 2007. An Assessment of the Intergovernmental Panel on Climate Change. IPCC Plenary XXVII, Spain:

http://www.ipcc.ch/pdf/assessment-report/ar4/syr/ar4_syr.pdf (accessed February 2012).

International Commission On Large Dams (ICOLD), 2003, World register of dams. http://www.icold-cigb.org (accessed February 2012).

Khalil, M. A. K., and Rasmussen, R. A., 1983. Sources, sinks, and seasonal cycles of atmospheric methane. Journal of Geophysical Research, v. 88, pp. 5131-5144.

Lima, I. B. T., Ramos, F. M., Bambace, L. A. W., and Rosa, R. R., 2008. Methane emissions from large dams as renewable energy resources: A developing nation perspective. Mitigation and Adaptation Strategies for Global Change, v. 13, pp. 193–206.

Long, K. D., Flanagan, L. B., and Cai, T., 2010. Diurnal and seasonal variation in methane emissions in a northern Canadian peatland measured by eddy covariance. Global Change Biology, v. 16, pp. 2420-2435.

McGinnis, D. F., Greinert, J., Artemov, Y., Beaubien, S. E., and Wüest, A., 2006. The fate of rising methane bubbles in stratified waters: How much methane reaches the atmosphere? Journal of Geophysical Research, v. 111, C09007.

Schleswig-Holstein Agency for Coastal Defense, National Park and Marine Conservation, 2011. Pers. Comm. Hans-Jürgen Weber and http://www.umweltdaten.landsh.de/public/hsi/index.html (accessed frequently in 2011).

Seeberg-Elverfeldt, J., Schlüter, M., Feseker, T., and Kölling, M., 2005. Rhizon sampling of porewaters near the sediment-water interface of aquatic systems. Limnology and Oceanography: Methods, v. 3, pp. 361-371.

Sebacher, D. I., Harriss, R. C., and Bartlett, K. B., 1985. Methane emissions to the atmosphere through aquatic plants. Journal of Environmental Quality, v. 14, pp. 40-46.

Schmale, O., Schneider von Deimling, J., Gülzow, W., Nausch, G., Waniek, J. J., and Rehder, G., 2010. Distribution of methane in the water column of the Baltic Sea. Geophysical Research Letters, v. 37, L12604.

Scranton, M. I., and McShane, K., 1991. Methane fluxes in the southern North Sea: the role of European rivers. Continental Shelf Research, v. 11, no. 1, pp. 37-52.

Stumm, W., and Morgan, J. J., 1996, Aquatic Chemistry: Chemical Equilibria and Rates in Natural Waters, Third Edition: New York, John Wiley & Sons, Inc., pp. 241-243.

Swinnerton, John W., Linnenbom, V. J., and Cheek, C. H., 1969. Distribution of methane and carbon monoxide between the atmosphere and natural waters. Environmental Science & Technology 3, no. 9, pp. 836-838.

Wiesenburg, D. A. and Guinasso Jr., N. L., 1979. Equilibrium solubilities of methane, carbon monoxide, hydrogen in water and seawater. Journal of Chemical and Engineering Data, v. 24, pp. 356–360.

Wilkniss, P. E., Lamontagne, R. A., Larson, R. E., and Swinnerton, J. W., 1978. Atmospheric trace gases and land and sea breezes at the Sepik River Coast of Papua, New Guinea. Journal of Geophysical Research, v. 83, no. C7, pp. 3672-3674.

Wuebbles, D.J. and Hayhoe, K., 2002. Atmospheric methane and global change. Earth-Science Reviews, v. 57, pp. 177-210.

Zimmerman, P. R., 1977. Determination of emission rates of hydrocarbons from indigenous species of vegetation in the Tampa/St. Petersburg, Florida area: Tampa Bay area photochemical oxidant study. U.S. EPA Report 904/9-77-028.